Quantification of the Uncertainties for the Space Launch System Liftoff/Transition and Ascent Databases

Amber L. Favaregh* and Heather P. Houlden†
ViGYAN, Hampton, Virginia, 23666

Jeremy T. Pinier‡
NASA Langley Research Center, Hampton, Virginia, 23681

A detailed description of the uncertainty quantification process for the Space Launch System Block 1 vehicle configuration liftoff/transition and ascent 6-DOF aerodynamic databases is presented. These databases were constructed from wind tunnel test data acquired in the NASA Langley Research Center 14- by 22-Foot Subsonic Wind Tunnel and the Boeing Polysonic Wind Tunnel in St. Louis, MO, respectively. The major sources of error for these databases were experimental error and database modeling errors.

Nomenclature

BMC	= balance moment center
C_Q	= value of force or moment coefficient obtained by querying the database
C_{DB}	= database value of force or moment coefficient at nominal breakpoints
C_{TRUE}	= the true value of the coefficient *C*
C_{WT}	= force or moment coefficient value acquired during wind tunnel testing
CAF	= body axis axial force coefficient
CLLF	= body axis rolling moment coefficient
CLMF	= body axis pitching moment coefficient
CLNF	= body axis yawing moment coefficient
CN, CNF	= body axis normal force coefficient
CY, CYF	= body axis side force coefficient
C_x	= force or moment coefficient value
D	= prefix for coefficient residuals
d_2	= bias correction factor for converting the mean range to an estimate of population standard deviation
DB	= database
DOF	= degrees of freedom
h/L	= height of vehicle above launch pad, normalized by tower height
LaRC	= Langley Research Center
MRP	= moment reference point
R	= range (maximum value – minimum value)
$\overline{R}$	= average range
Re	= Reynolds number
SLS	= Space Launch System
STDEV	= standard deviation
U_{bal}	= balance calibration fit uncertainty
$U_{C,Q}$	= uncertainty associated with database query
U_{DBM}	= database modeling uncertainty
U_{DBMnet}	= net database modeling uncertainty
$U_{DBMnet,Ascent}$	= net ascent database uncertainty

* Senior Aerospace Engineer, 30 Research Drive, Hampton, VA 23666, Senior Member
† Senior Aerospace Engineer, 30 Research Drive, Hampton, VA 23666, Senior Member
‡ Research Aerospace Engineer, Configuration Aerodynamics Branch, MS 499, Associate Fellow

$U_{DBMnet,Tower}$ = net tower increments uncertainty
$U_{DBMnet,Trans}$ = net transition database uncertainty
U_{DB} = total database uncertainty
$U_{DB,Ascent}$ = total ascent database uncertainty
$U_{DB,Tower}$ = total tower increments uncertainty
$U_{DB,Trans}$ = total transition database uncertainty
U_{EXP} = experimental uncertainty
$U_{EXP,Ascent}$ = experimental uncertainty for ascent test data
$U_{EXP,Tower}$ = experimental uncertainty for tower effects test data
$U_{EXP,Trans}$ = experimental uncertainty for transition test data
UF = uncertainty factor
UQ = uncertainty quantification
WT = abbreviation for wind tunnel
α = angle of attack in body coordinates (degrees)
β = angle of sideslip in body coordinates (degrees)
σ_{rep} = standard deviation for experimental within-test repeatability

I. Introduction

A statement of uncertainty should be included with any aerodynamic database. The statement should include the effects of all of the significant sources of uncertainty. In this paper, the queried (user-interpolated) value in the database response surfaces for any of the six aerodynamic force and moment coefficients is designated as C_Q. Then the true value, C_{TRUE}, is defined in Eq. (1), where $U_{C,Q}$ is the estimated uncertainty bound for C_Q.

$$C_Q - U_{C,Q} \le C_{TRUE} \le C_Q + U_{C,Q} \tag{1}$$

This paper presents a description of the uncertainty modeling of the Space Launch System (SLS) liftoff/transition and ascent aerodynamics 6-DOF databases. Uncertainty bounds were estimated for all processes used to acquire the data and to modify these data during database construction. This includes wind tunnel repeatability errors and database modeling errors. Wind tunnel bias error was not included as it was assumed to be negligible. The individual uncertainties were combined by the root-sum-square (RSS) method. It was also assumed that the errors are samples from a random variable and that errors from different sources are independent and uncorrelated.

The SLS liftoff/transition and ascent databases were both constructed using wind tunnel data. The data used for the liftoff/transition database were acquired during wind tunnel tests conducted in the NASA Langley Research Center 14- by 22-Foot Subsonic Wind Tunnel (SWT) on a 1.75%-scale model. The ascent database was constructed from data obtained in the Boeing Polysonic Wind Tunnel (PSWT) on a 0.8%-scale model. Data from the PSWT test were obtained at Mach numbers from 0.5 to 5.0.

II. Description of SLS Liftoff/Transition and Ascent Aerodynamic Databases

The liftoff/transition database defines the aerodynamics of the launch vehicle from liftoff through the transition from high to low angle-of-attack flight at low subsonic Mach numbers. The liftoff/transition database contains two data tables. One table contains the baseline aerodynamic coefficients from liftoff through transition and is a function of angle-of-attack and sideslip. The angles of attack and sideslip in the transition database vary from -90° to +90°. The other table contains increments of the effects due to the presence of the launch tower as the height of the vehicle from the launch pad increases immediately after liftoff. A photograph of the SLS model mounted next to the launch tower is shown in Figure 1 and illustrates the test setup for measuring the effects of the launch tower on the vehicle.

The tower effects increments are a function of the relative height of the vehicle above the launch pad (h/L) and wind azimuth angle. Figure 2 depicts increasing h/L as the vehicle lifts off the launch pad, and Figure 3 shows the orientation of wind azimuth angles with respect to the tower. During the tower effects portion of the wind tunnel test, data were acquired with the model at varying wind azimuth angles and h/L values. The effect of the tower on the vehicle is presumed to be negligible by the time the relative height of the vehicle is h/L=1.2. Thus, the h/L breakpoints in the tower effect increments table vary from 0.0 to 1.2. The tower effect increments were computed by subtracting wind tunnel data measured on the vehicle by itself from the data measured on the vehicle in the

presence of the tower. There was a physical limitation of the turntable, which prevented it from rotating more than 340°. The vehicle and launch tower models were installed in the test section such that this twenty degree gap was located at wind azimuth angles of 80° to 100°. Therefore, no data were acquired at azimuth angles of 80° to 100°. Data at these angles was filled in by mirroring data from the opposite wind azimuth (West wind in Figure 3).

The transition database was constructed using data acquired on the vehicle alone in the NASA LaRC 14- by 22-Foot SWT.[1] These data were acquired as pitch sweeps at different roll angles and roll sweeps at several pitch angles. Response surfaces were then built for each aerodynamic coefficient using a three-dimensional smoothing spline[2] to fit the wind tunnel data. Figure 4 shows the transition database breakpoint values, in terms of total angle of attack and roll angle. Figure 4 also displays the total angle of attack and roll angle wind tunnel set point values used to construct the database response surfaces. A requirement for the SLS aerodynamic databases is that they be defined as functions of α and β. So the desired angle of attack and sideslip database breakpoint values were converted to total angle of attack and roll values (the black dots in Figure 4), and then response surfaces were interrogated at these values.

The ascent database defines the aerodynamic forces and moments for the phase of flight that follows transition.[3] This flight regime covers small angles of attack and Mach numbers ranging from 0.5 through 5.0. The ascent database is a function of angle of attack, sideslip angle, and Mach number. Wind tunnel test data acquired in the Boeing PSWT was used to construct the ascent database for the SLS configuration. As with the liftoff/transition wind tunnel test, the PSWT ascent data were acquired from pitch sweeps at fixed roll angles and roll sweeps at fixed pitch angles. Response surfaces were constructed for each aerodynamic coefficient at every Mach number tested. The desired ascent database α and β breakpoint values were converted to total angle of attack and roll values, and the individual response surfaces were interrogated at the these values. Figure 5 shows the total angle of attack and roll coordinates for the ascent test data, and the ascent database total angle of attack and roll breakpoint values.

III. General Description of Database Uncertainty Modeling

For these databases, which were developed using only experimental data, the uncertainty is composed generally of:

1. Experimental error associated with the adjusted wind tunnel dataset used to build the database response surface (i.e., wind tunnel data repeatability, U_{EXP}).

2. Curve-fit error associated with creating the database response surface from the computational dataset or the adjusted experimental dataset (database modeling error, U_{DBM}).

3. Wind tunnel balance calibration fit error (U_{bal}).

A general expression of the database uncertainty buildup is described in Eq. (2). The total uncertainty $U_{C,Q}$ is obtained by root-sum-squaring the individual error components.

$$U_{C,Q}^2 = U_{EXP}^2 + U_{DBM}^2 + U_{bal}^2 \tag{2}$$

A discussion of these uncertainties and how they are quantified for both the liftoff/transition and ascent databases is presented in the following sections. The general approach to quantifying launch vehicle aerodynamic database uncertainties was developed and implemented during the Ares I program.[4-5] All analyses presented in this paper were performed on body axis coefficients and at the balance moment center. The pitching and yawing moment uncertainties were then transferred to the moment reference point for use with the database. Instructions on transferring the pitching and yawing moment database uncertainties from the moment reference point to a nominal center of gravity were provided to the database users as part of the implementation instructions.

IV. Experimental Uncertainties

Dating back to the Ares I program, it has been standard practice to acquire repeat runs during every wind tunnel test so that the experimental error can be quantified and included in the overall uncertainties for each database. An analysis was performed on groups of replicate runs obtained during each wind tunnel test in order to quantify the within-test repeatability (σ_{rep}) for each test. For each set of replicate runs, the data were interpolated to nominal

angles. During the test in the 14- by 22-Foot SWT, the data were acquired in pitch-pause mode. To remove any set point errors from this style of testing, the data were interpolated to nominal set point values. The SWT is very accurate in setting the desired angles, so this interpolation was minimal. In the Boeing PSWT, data were acquired continuously during each pitch or roll sweep, so the interpolation was done to produce a more discretized set of data for each run. For each set of repeat data points, the absolute value of the difference (i.e., range, R) between the replicate points was computed and normalized by the bias correction factor d_2, to obtain an estimate of the standard deviation as shown in Eq. (3).[6] This results in a separate normalized range for each set of repeat points.

$$\sigma_{rep} = \frac{R}{d_2} \tag{3}$$

Then these values of σ_{rep} are plotted and evaluated to determine if the repeatability is a function of any of the independent variables or if the repeatability values can be pooled together over a range of values. The 3-sigma bounds for U_{EXP} is estimated by setting the bounds to capture 99.7% of the σ_{rep} values.

A. Liftoff/Transition Wind Tunnel Test U_{EXP}

There were two phases of the wind tunnel test conducted in the NASA LaRC 14- by 22-Foot wind tunnel, and repeat runs were acquired during both phases of the test. One phase was the transition portion of the test, where all the data were acquired entirely in the pitch plane. During this portion of the test, data were acquired as pitch or roll sweeps, for total angles of attack from -10° to +90° and roll angles of -180° to +180°. The tower effects portion of the test was conducted with the vehicle model and a scaled model of the launch pad and tower mounted on a turntable in the floor of the test section. During this portion of the test, the model set points were wind azimuth angle and relative vehicle height, h/L. Consequently, separate experimental uncertainty bounds for the transition and tower effects portions of the test were computed.

For example, a plot of the transition test CNF σ_{rep} values versus total angle of attack is shown in Figure 6. Different color symbols were used for pitch and roll run replicates to show that there was no significant difference in the repeatability of roll and pitch runs. However, the repeatability of CNF for the transition phase of the test did vary somewhat with total angle of attack. So the repeatability values were pooled over four ranges of total angle of attack. The red dashed line in Figure 6 represents the UEXP 3-sigma bound for CNF. Repeatability values for total angles of attack from -10° to 20° and 35° to 50° were pooled together and the red dashed lines in these regions bound 99.7% of the repeatability values. The experimental uncertainty bounds were largest between 20° and 35° total angle of attack due to model dynamics that affected repeatability and limited the amount of data that could be acquired in this region. Since the transition test repeatability was a function of total angle of attack and the database a function of angle of attack and sideslip, it was necessary to convert the UEXP bounds (such as the dashed line in Figure 6) into three-dimensional bounds in α-β space. First, a table of the UEXP bounds in total angle of attack and roll angle space was generated, as shown in Figure 7. Then these bounds, defined in terms of total angle of attack and roll, were converted to α-β space, as displayed in Figure 8. This process was repeated for every aerodynamic coefficient.

For the tower effects phase of the wind tunnel test, data were acquired either as wind azimuth angle sweeps at a constant relative height (h/L) or h/L sweeps at a constant wind angle. Repeat runs for both types of runs were obtained. The repeatability for the tower effects portion of the test was computed using Eq. (3), and the results plotted versus wind azimuth angle and h/L. As an example, the tower effects repeatability for CYF is plotted versus relative height (h/L) in Figure 9, and plotted versus wind azimuth angle in Figure 10. Note in Figure 10 that there are no data for azimuth angles between 80° and 100° due to the previously mentioned physical limitations of the turntable.

To quantify the total experimental uncertainty associated with the SLS tower effects increments, the experimental uncertainty 3-sigma limits were computed using Eq. (4), where n=2 because the tower effects were obtained by combining (through subtraction) two terms from the test data. Thus, the experimental repeatability must be counted twice in estimating the total experimental uncertainty.

$$U_{EXP} = \sqrt{n\left(3\sigma_{rep}\right)^2} = 3\sqrt{n}\sigma_{rep} \tag{4}$$

Therefore, the contribution of experimental error to the SLS tower effects database uncertainty is defined as follows:

$$U_{EXP,Tower} = 3\sqrt{2}\sigma_{rep} \tag{5}$$

B. Ascent Wind Tunnel Test U_{EXP}

There were numerous pairs of replicate runs obtained at every Mach number tested during the ascent test conducted in the Boeing PSWT. Repeat runs were obtained for both pitch and roll runs. The ascent testing was conducted at small pitch angles, so the repeatability only varied with Mach number. Values of σ_{rep} were computed using Eq. (3) for every set of ascent repeat runs and then grouped according to Mach number. The 99.7th percentile bounds on σ_{rep} were computed at each Mach number to estimate U_{EXP} for the ascent database experimental uncertainty term. This was done for each force and moment coefficient. Figures 11-13 show summaries of the SLS ascent repeatability and experimental uncertainty bounds for CNF, CAF, and CYF, respectively. The solid red lines in the figures represent the 3-sigma experimental uncertainty bounds for each coefficient.

V. Database Modeling Errors

Database modeling errors include all errors introduced in constructing a database response surface at canonical inference space points, from an experimental or CFD input dataset. Example sources of database modeling errors are:

1. smoothing and/or curve-fitting of the input dataset
2. assumptions used to create reduced-order models from sparse input data, in order to fill out the database inference space
3. use of symmetry, mirroring, etc.

The process for estimating the database modeling uncertainty is to compute the absolute difference between the database queried at the wind tunnel set point values and the original wind tunnel data values, as described in Eq. (6). The residuals are examined to determine if they are a function of Mach number or model attitude, and 3-sigma bounds (U_{DBM}) were estimated by computing the 99.7th percentile of the residuals.

$$DC_x = |C_{DB} - C_{WT}| \tag{6}$$

Since the experimental errors were already accounted for using Equations (3) and (4), it is necessary to remove the experimental uncertainty from the database modeling uncertainty, UDBM, so as not to exaggerate the modeling errors by "double counting" the repeatability. This is referred to as the net database modeling error because it represents just the errors associated with the process of constructing the database (i.e., smoothing, averaging, mirroring, interpolation, etc.). The net database modeling uncertainty is computed using Eq. (7), with the caveat that U_{DBMnet}=0 if the U_{EXP} exceeds U_{DBM}.

$$U_{DBMnet} = \sqrt{U_{DBM}^2 - U_{EXP}^2} \tag{7}$$

A. Transition and Tower Effects Database

The SLS transition database modeling residuals were computed for each aerodynamic coefficient and 3-sigma bounds were estimated. Plots of the modeling residuals and subsequent database modeling uncertainty bounds are presented in Figures 14-19. The residuals varied with total angle of attack for all coefficients except CAF (Figure 15). For the other five coefficients, the residuals were pooled over ranges of total angle of attack and the bounds estimated for each region. Since the database modeling bounds were a function of total angle of attack they were converted to α-β space in the same manner as the transition test experimental uncertainty bounds. The resulting transition database modeling uncertainty bounds expressed in terms of α and β are presented in Figures 20-25. The net database modeling uncertainty is computed by subtracting out the transition test experimental uncertainty, as shown in Eq. (8).

$$U_{DBMnet,Trans} = \sqrt{U_{DBM,Trans}^2 - U_{EXP,Trans}^2} \tag{8}$$

Equation (9) shows how the total transition database uncertainty is computed, where U_{bal} is the balance calibration fit uncertainty. The term UF in Eq. (9) is an uncertainty factor, which is intended to account for other known or unknown factors that may not be modeled in the database. Examples of this could be incomplete configuration information, or changes made to the geometry since the data were acquired (e.g., modifications to protuberances, addition/removal of protuberances, changes to fairings or other hardware). Even relatively small changes to the outer mold lines can affect the aerodynamics of the vehicle.

$$U_{DB,Trans} = UF_{Trans}\sqrt{U^2_{DBMnet,Trans} + U^2_{EXP,Trans} + U^2_{bal}} \tag{9}$$

For the tower effects increments, the modeling uncertainty was generally smaller than the experimental uncertainty, because little to no modeling was done. The vehicle alone data were simply subtracted from the vehicle with tower data. So throughout most of the tower increment database the net database modeling uncertainty was zero. However, for wind azimuth angles of 80° to 100°, a process of mirroring data and averaging was used to compute tower increments for wind angles of 80° to 100°. Data obtained at wind azimuth angles from 250° to 290° were mirrored over to azimuth angles of 70° to 110°. One set of mirrored data was anchored at 70° and another set of mirrored data was anchored at 110°. These two sets of mirrored data were averaged and used to compute the tower increments at azimuth wind angles from 80° to 100°. In order to estimate uncertainties for the 80° to 100° tower increments, two "alternate" sets of increments were computed. One alternate set of increments was computed using the mirrored data anchored at 70°. The other alternate set was computed using the mirrored data anchored at 110°. A sample plot of this process is shown in Figure 26. The maximum difference between the final database tower increments and the alternate increments was set as the modeling error for wind azimuth angles 80° to 100°. Then the total database uncertainty for the tower effects increments was computed using Eq. (10).

$$U_{DB,Tower} = UF_{Tower}\sqrt{U^2_{DBMnet,Tower} + U^2_{EXP,Tower} + U^2_{bal}} \tag{10}$$

Plots of the tower increments database uncertainty buildup are presented in Figures 27-32. For each aero coefficient, the modeling residuals, database modeling uncertainty bounds, experimental uncertainty bounds (from Eq. (5)), and total database uncertainty (from Eq. (10)) are plotted against wind azimuth angle. Notice in Figure 27 that the experimental uncertainty exceeds the modeling uncertainty for all azimuth angles except from 80° to 100°. Similar plots for the remaining five aero coefficients are shown in Figures 28-32.

B. Ascent Database

The SLS ascent database modeling residuals were computed for each aerodynamic coefficient and every Mach number. Then 3-sigma bounds were computed at each Mach number. Plots of the ascent database modeling residuals, along with the subsequent modeling uncertainty bounds ($U_{DBM,Ascent}$) and ascent experimental uncertainty bounds ($U_{EXP,Ascent}$), are presented in Figures 33-38. The total database modeling uncertainty is computed using Equations (11) and (12).

$$U_{DBMnet,Ascent} = \sqrt{U^2_{DBM,Ascent} - U^2_{EXP,Ascent}} \tag{11}$$

$$U_{DB,Ascent} = UF_{Ascent}\sqrt{U^2_{DBMnet,Ascent} + U^2_{EXP,Ascent} + U^2_{bal}} \tag{12}$$

Note in the figures that many of the residuals lie outside the experimental uncertainty bounds. This indicates that the uncertainties associated with smoothing the data and combining smoothed and fitted pitch and roll run data

generally exceeded the experimental uncertainty (i.e., wind tunnel repeatability). If the database modeling residuals mostly fell below the experimental uncertainty bounds, then the database modeling errors would be considered insignificant, and the experimental and database interpolation errors would be the only sources of uncertainty for the wind tunnel-derived database.

The database modeling residuals lie within the experimental uncertainty bounds at the lowest Mach numbers for every coefficient except pitching and yawing moment. At these Mach numbers, the database modeling errors are insignificant and the net database modeling uncertainty term becomes zero.

VI. Concluding Remarks

A detailed uncertainty analysis was developed for the Space Launch System Block 1 configuration ascent and liftoff/transition aerodynamic 6DOF databases. These databases were constructed using wind tunnel data from two test facilities. The errors for each database were identified and quantified. The total uncertainty for each database was obtained by root sum squaring the individual uncertainty terms. The transition database uncertainties are defined in terms of α and β, while the tower effects increment uncertainties are expressed as a function of wind azimuth angle. The 6DOF ascent database uncertainties are simply a function of Mach number, as the ascent test data were acquired at low angles of attack and sideslip. In general, the total uncertainty for each database consists of experimental uncertainty (wind tunnel repeatability) and modeling uncertainty.

Acknowledgments

The authors wish to thank the Space Launch Systems experimental and database teams at Langley Research Center for providing the data for our analysis. The first two authors of this paper were funded under NASA contract NNL12AA09C.

References

1. Pinier, J.T., Erickson, G.E., Paulson, J., Tomek, W.G., Bennett, D.W., Blevins, J.A., "Space Launch System Liftoff and Transition Aerodynamic Characterization in the NASA Langley 14- by 22-Foot Subsonic Wind Tunnel", AIAA 2015-0775.
2. D'Errico, John R., "Understanding Gridfit", 2006.
3. Pinier, J.T., Bennett, D.W., Blevins, J.A., Erickson, G.E., Favaregh, N.M., Houlden, H.P., Tomek, W.G., "Space Launch System Ascent Static Aerodynamic Database Development", AIAA-2014-1254.
4. Hemsch, M.J., Hanke, J.L., Walker, E.L., and Houlden, H.P., "Detailed Uncertainty Analysis for Ares I Ascent Aerodynamics Wind Tunnel Database", AIAA-2008-4259.
5. Houlden, H.P., Favaregh, A.L., Hemsch, M.J., "Uncertainty Quantification and Modeling for Ares I A106 Ascent Aerodynamics Database", NASA/TM-2013-218045, 2013.
6. Montgomery, Douglas, C., *Introduction to Statistical Quality Control*, 3rd Ed., Wiley, 1996.

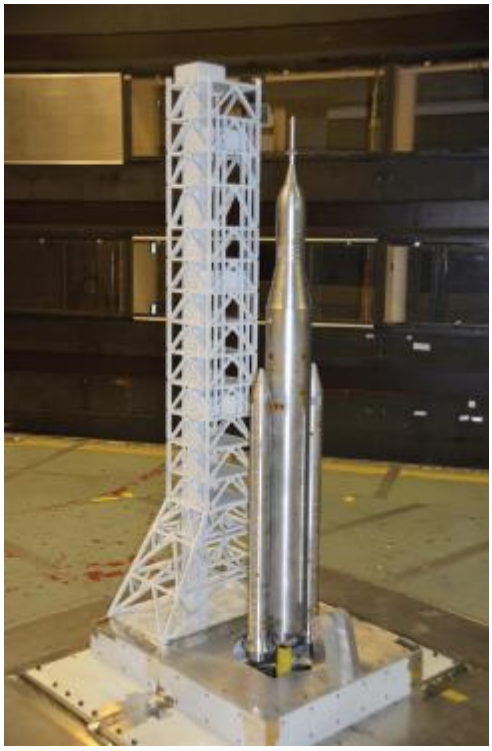

Figure 1. Photograph of model of SLS Block 1 vehicle and launch tower installed in the NASA LaRC 14- by 22-Foot Subsonic Wind Tunnel.

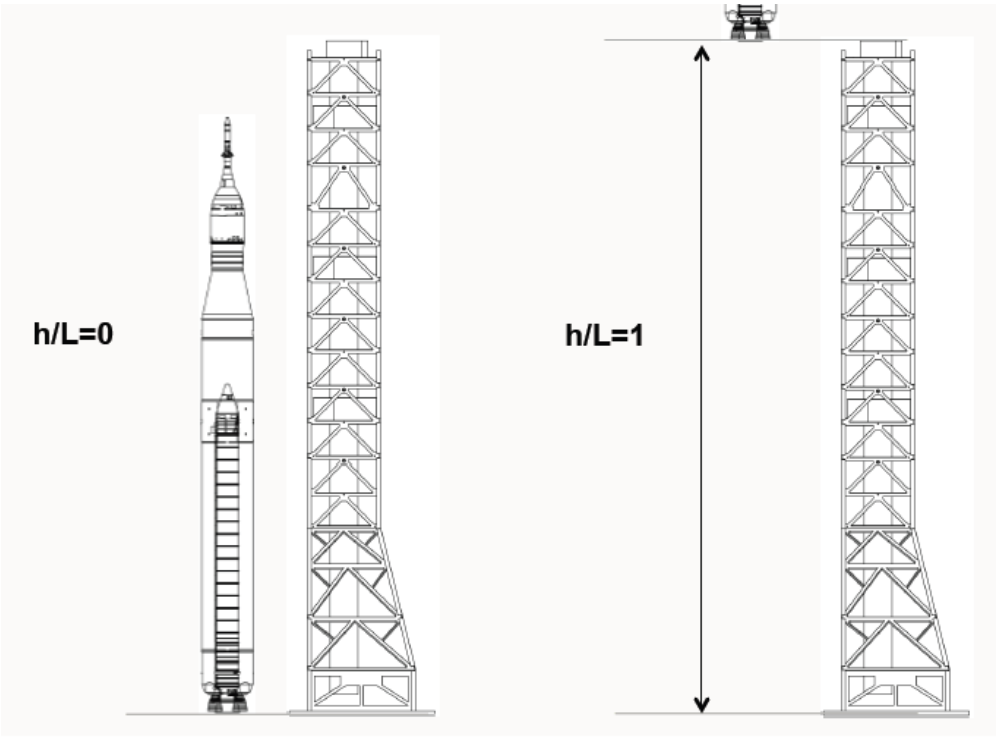

Figure 2. Depiction of increasing h/L as the vehicle lifts off from the launch pad. When the vehicle is sitting on the pad h/L=0.

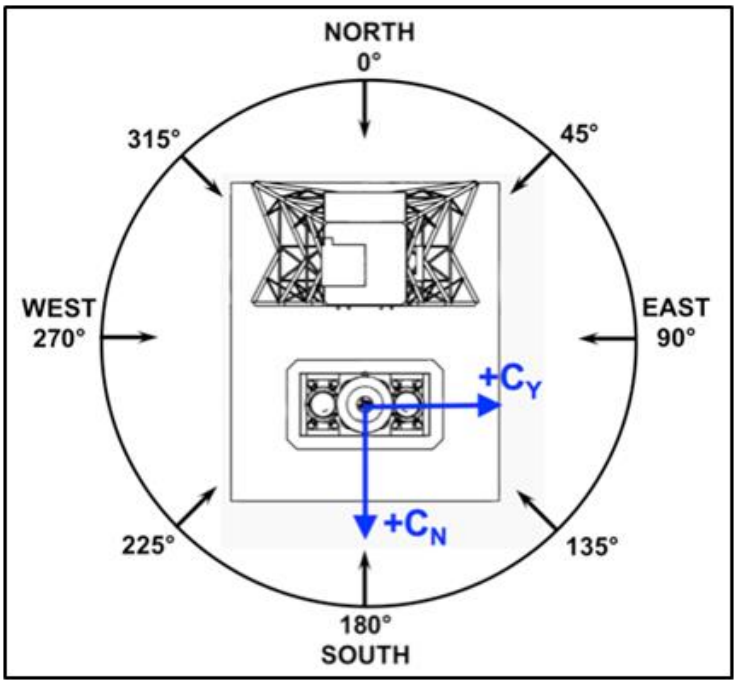

Figure 3. Definition of ground wind azimuth angle orientation.

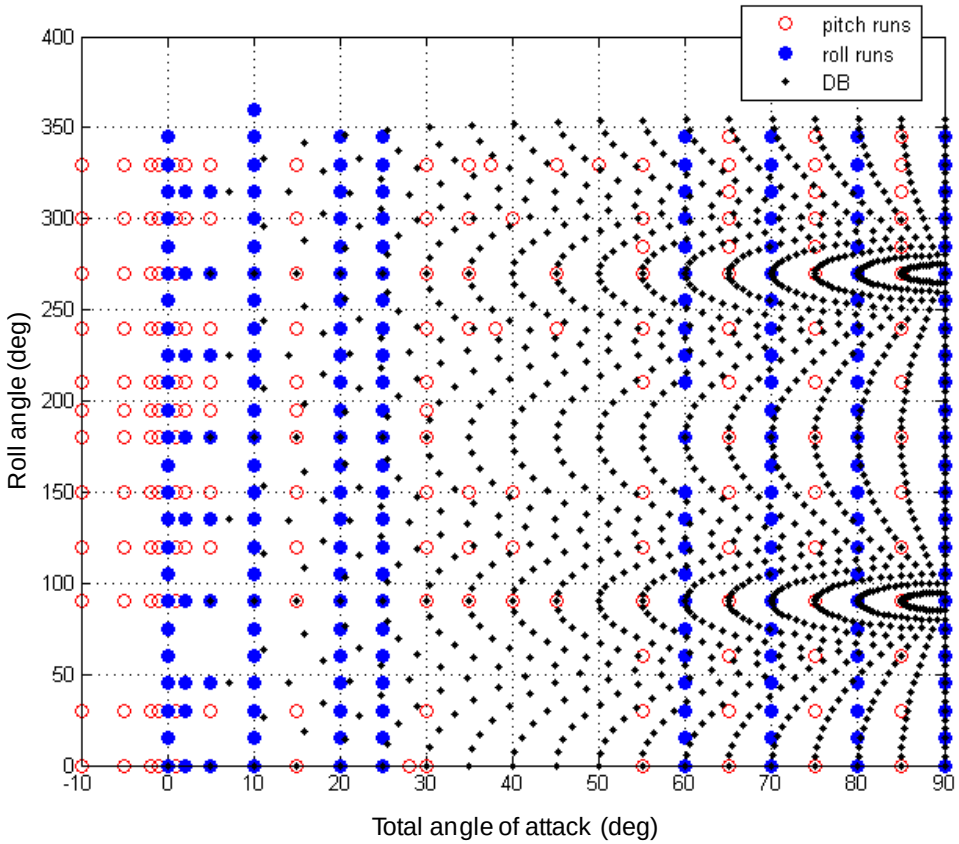

Figure 4. Comparison of total angle of attack and roll coordinates acquired during transition wind tunnel testing and pitch and roll coordinates of final transition database.

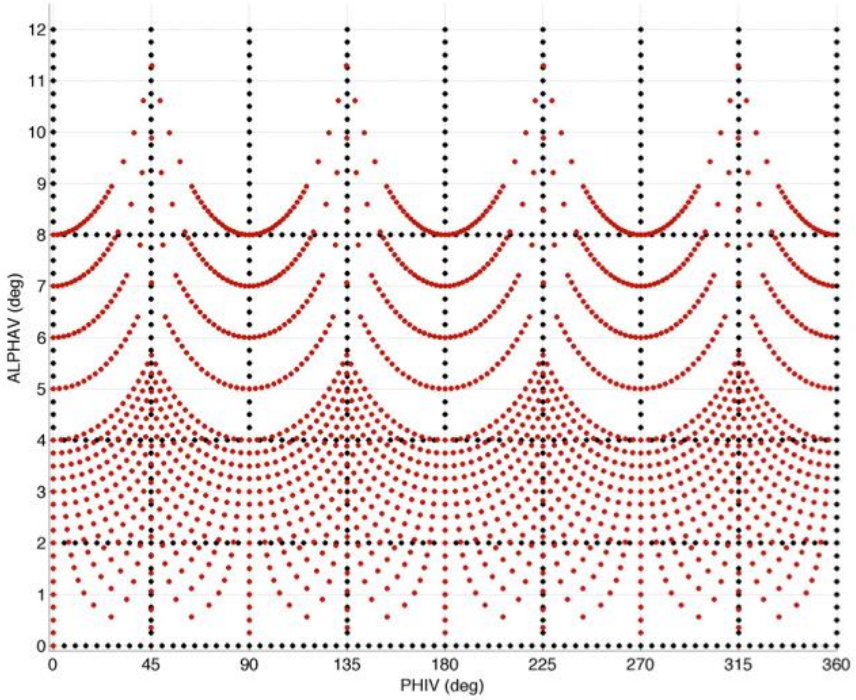

Figure 5. Wind tunnel test points (black dots) and database breakpoints (red dots) in total angle of attack and roll space.

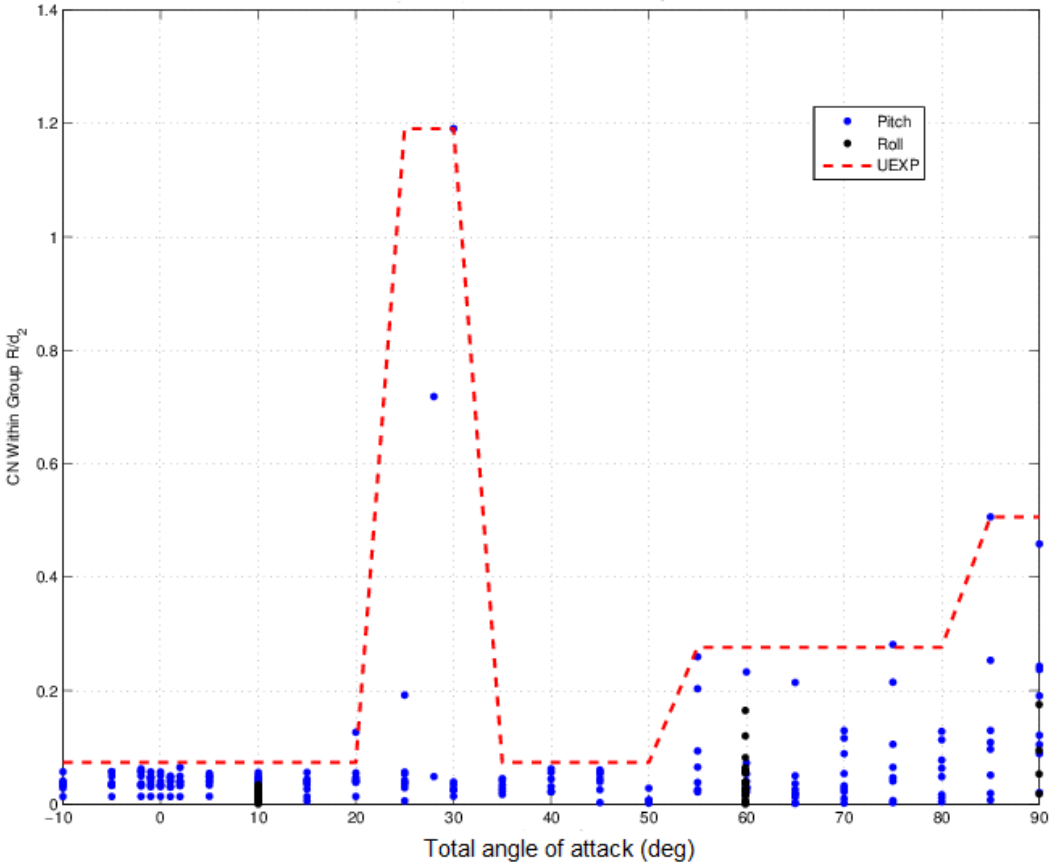

Figure 6. Transition test repeatability for CNF as a function of total angle of attack.

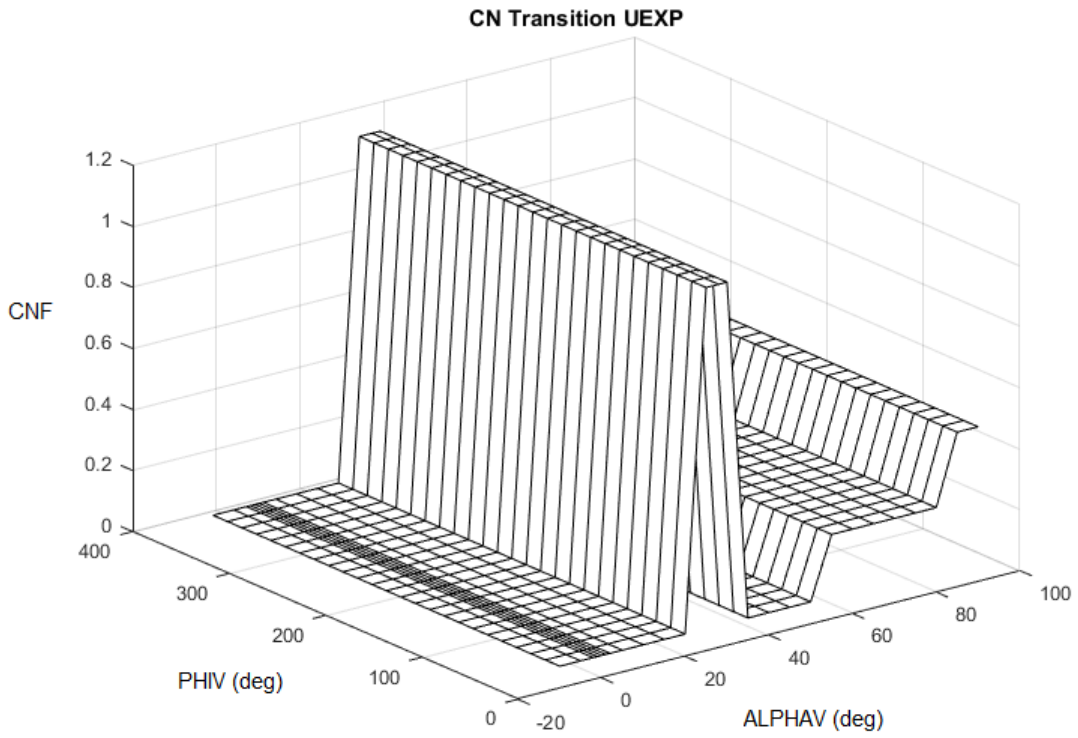

Figure 7. Transition test repeatability for CNF shown versus total angle of attack and roll angle.

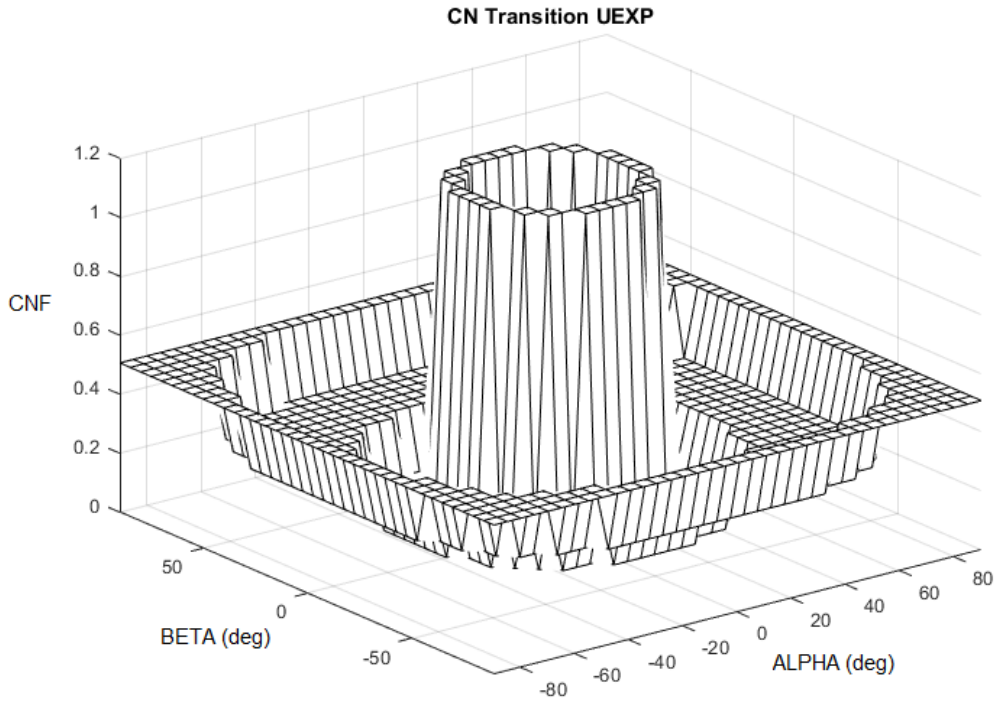

Figure 8. Transition test repeatability for CNF after converting total angle of attack and roll to α and β.

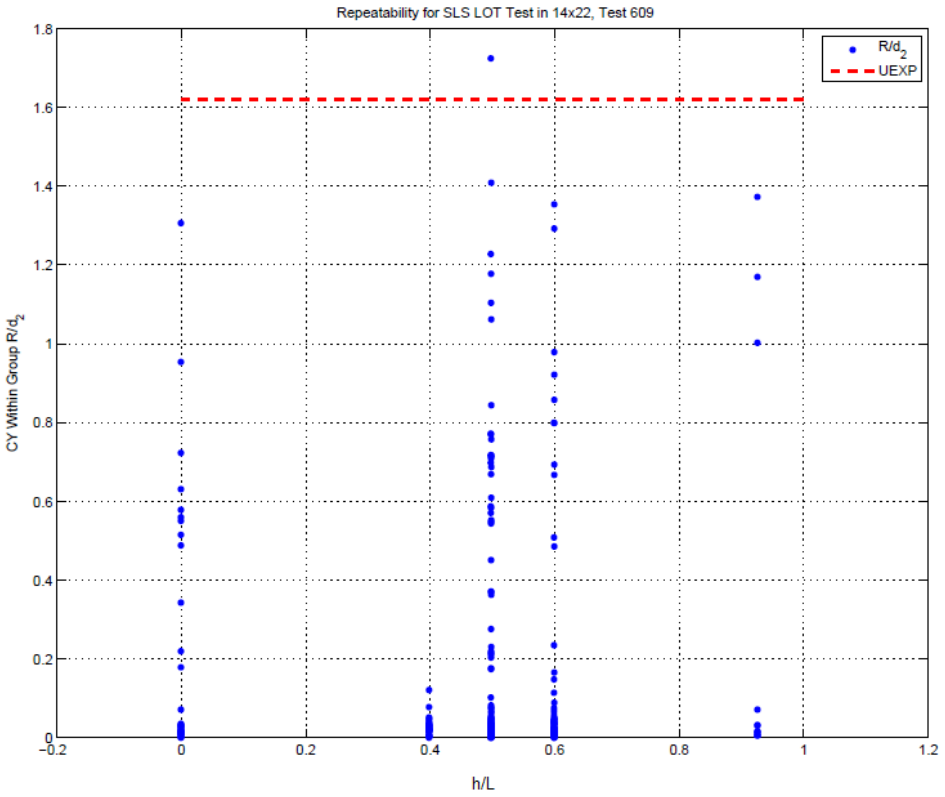

Figure 9. Tower effects test repeatability for CYF plotted versus wind relative vehicle height (h/L).

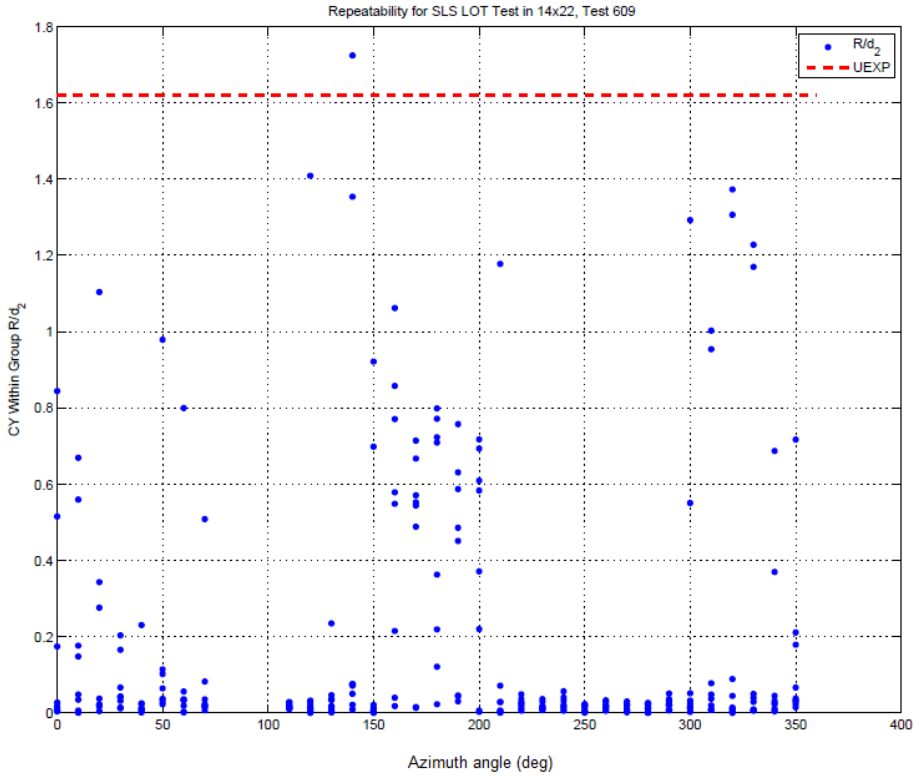

Figure 10. Tower effects test repeatability for CYF plotted versus wind azimuth angle.

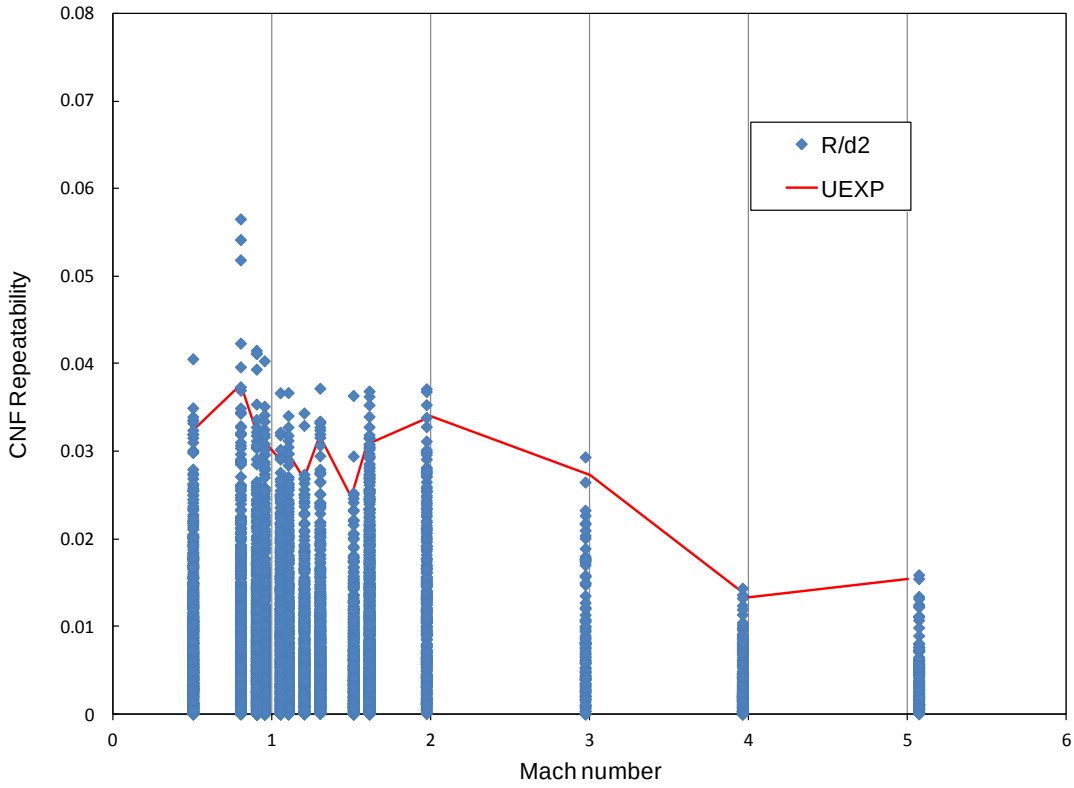

Figure 11. Effect of Mach number on CNF repeatability for Boeing PSWT ascent test data.

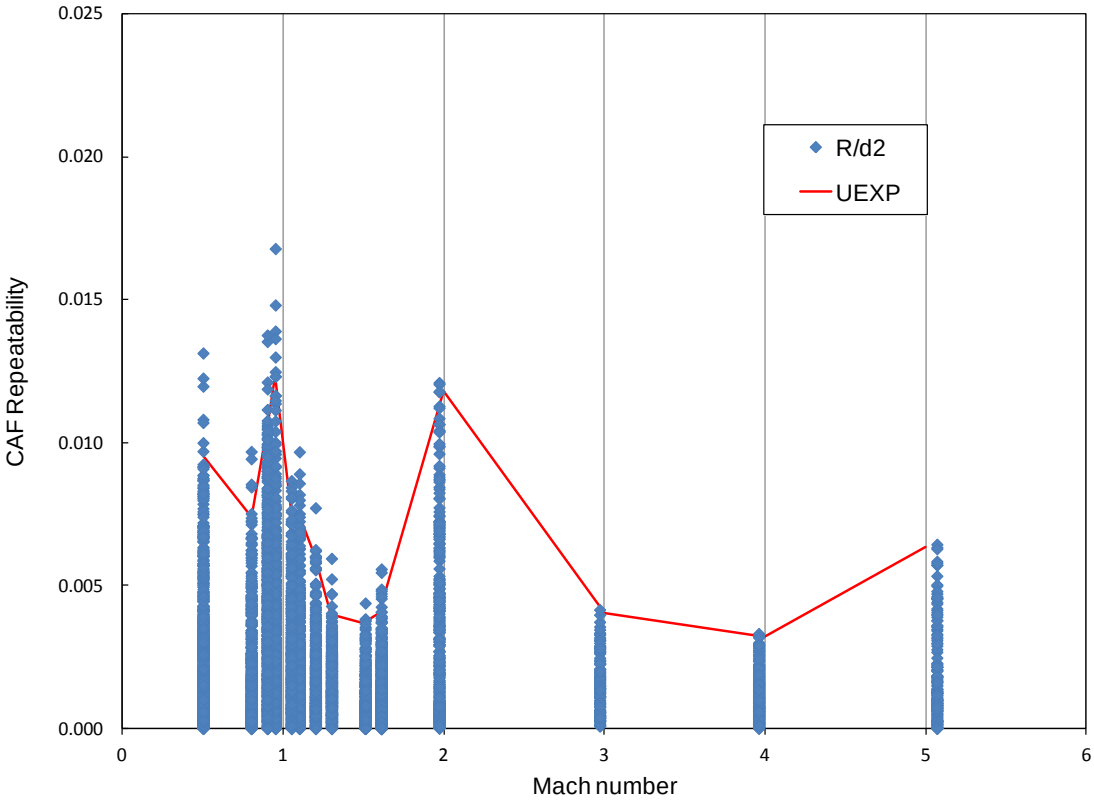

Figure 12. Effect of Mach number on CAF repeatability for Boeing PSWT ascent test data.

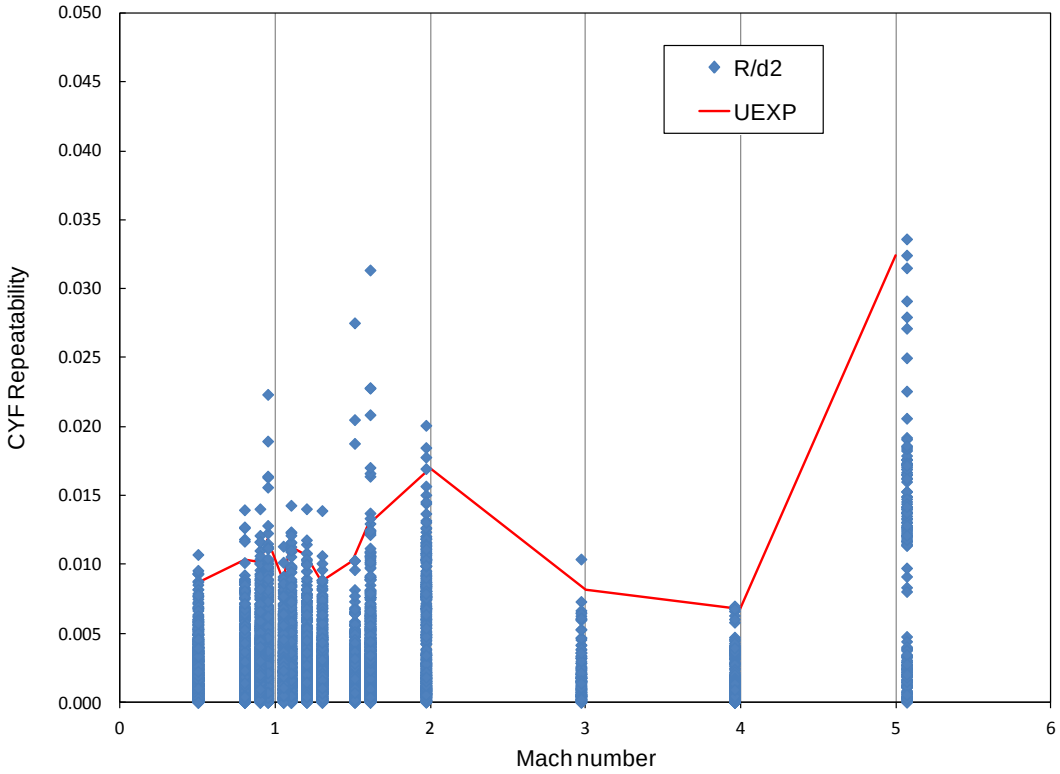

Figure 13. Effect of Mach number on CYF repeatability for Boeing PSWT ascent test data.

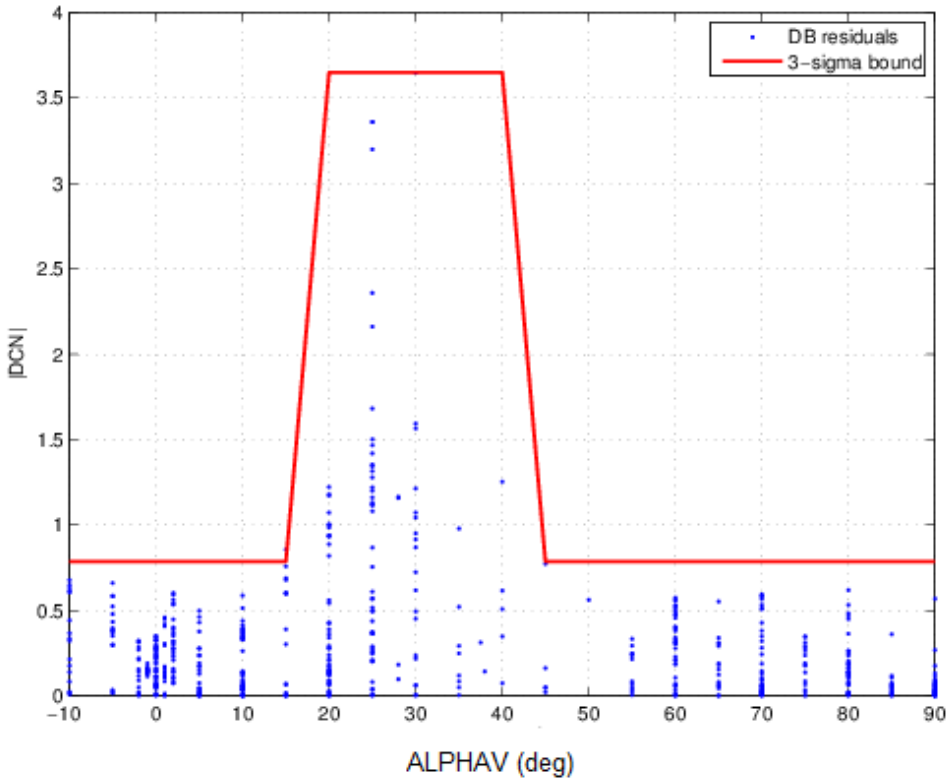

Figure 14. Transition database modeling residuals for CNF and 3-sigma bounds versus total angle of attack.

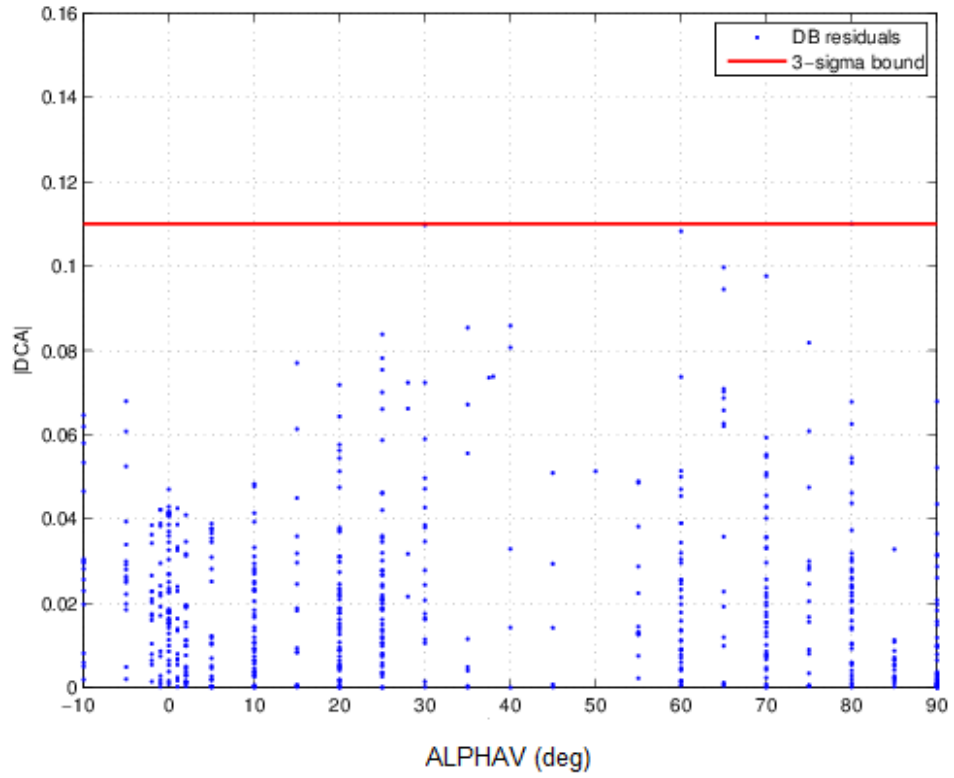

Figure 15. Transition database modeling residuals for CAF and 3-sigma bounds versus total angle of attack.

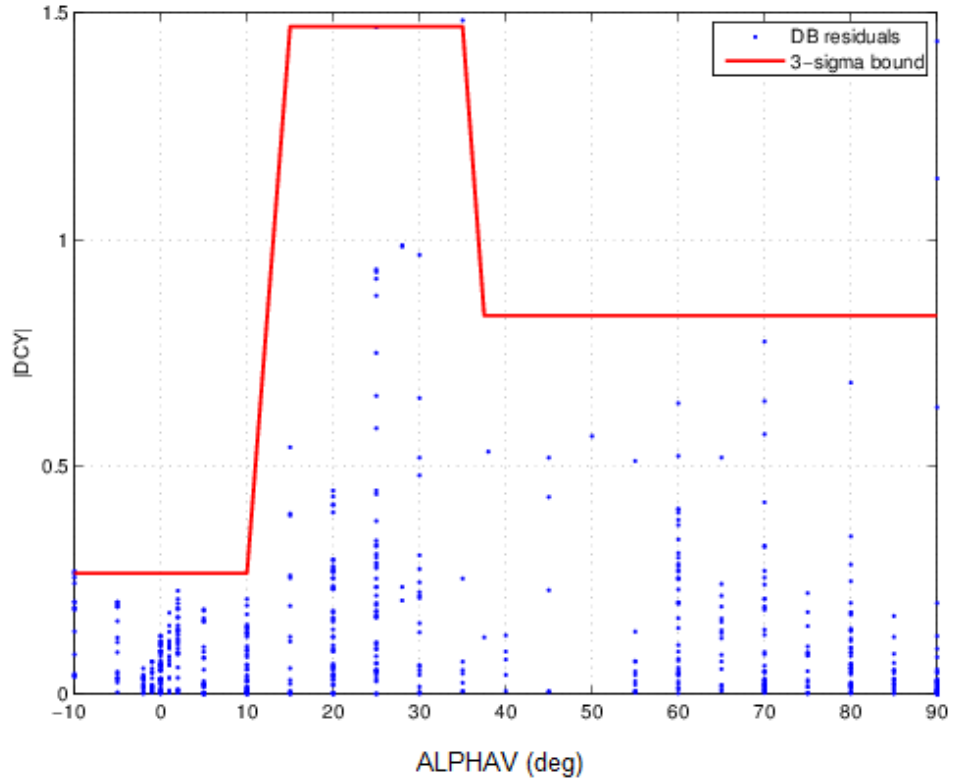

Figure 16. Transition database modeling residuals for CYF and 3-sigma bounds versus total angle of attack.

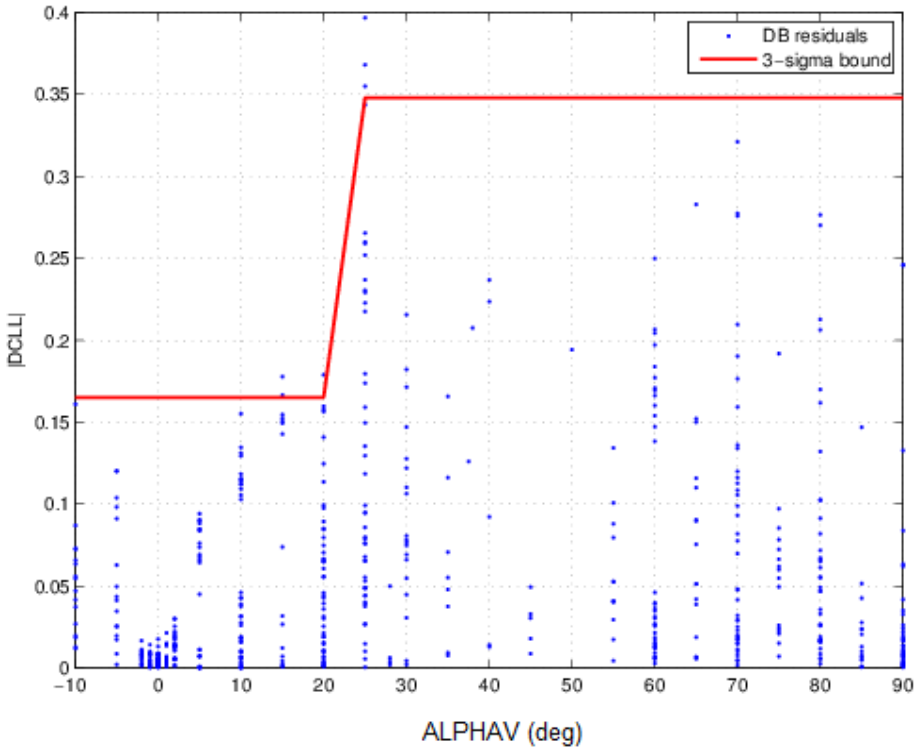

Figure 17. Transition database modeling residuals for CLLF and 3-sigma bounds versus total angle of attack.

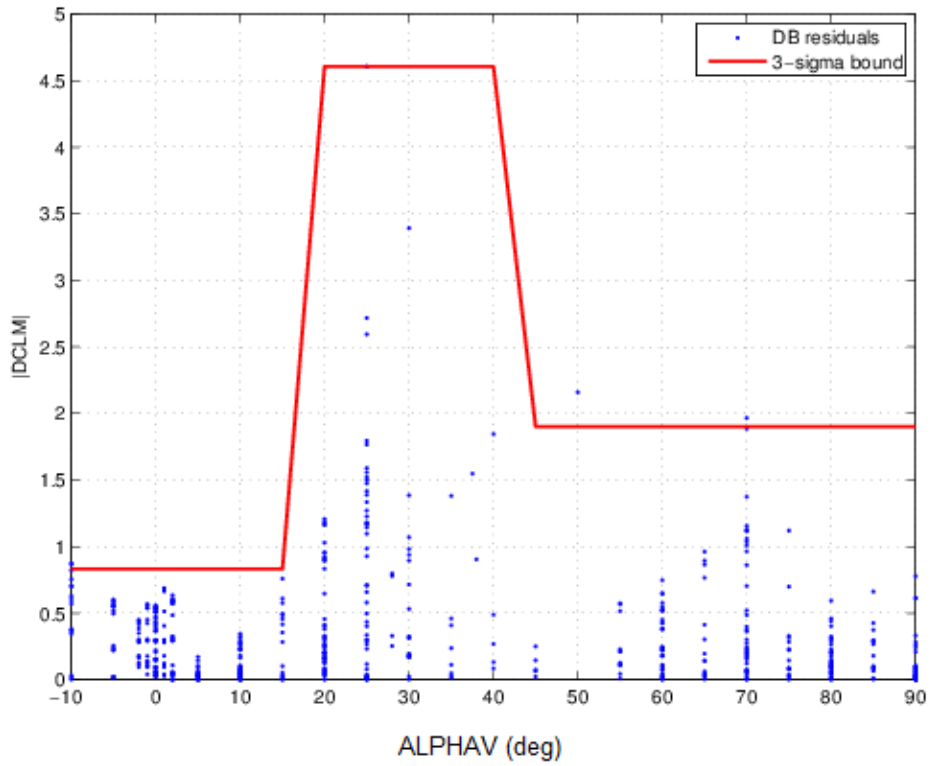

Figure 18. Transition database modeling residuals for CLMF and 3-sigma bounds versus total angle of attack.

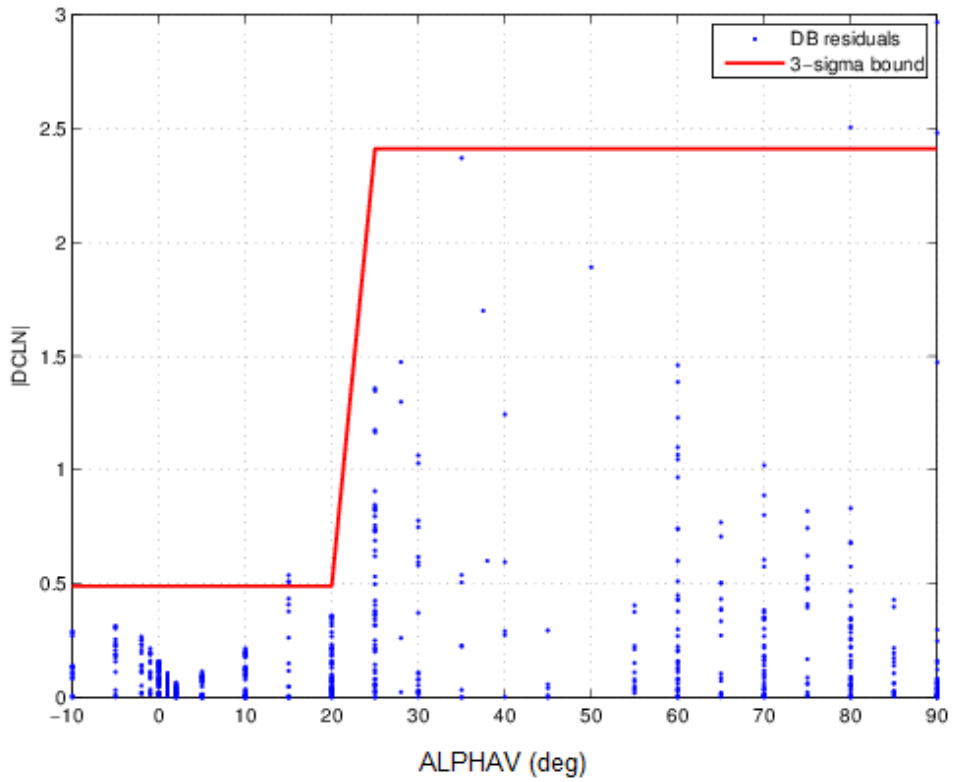

Figure 19. Transition database modeling residuals for CLNF and 3-sigma bounds versus total angle of attack.

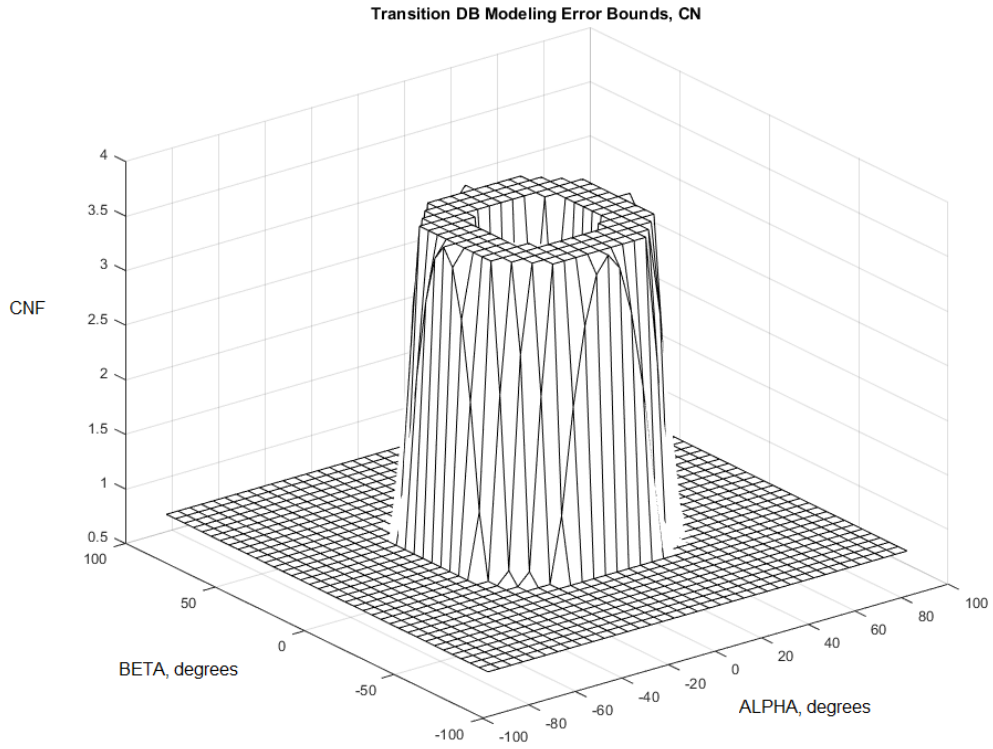

Figure 20. Transition database modeling error bounds for CNF in α-β space.

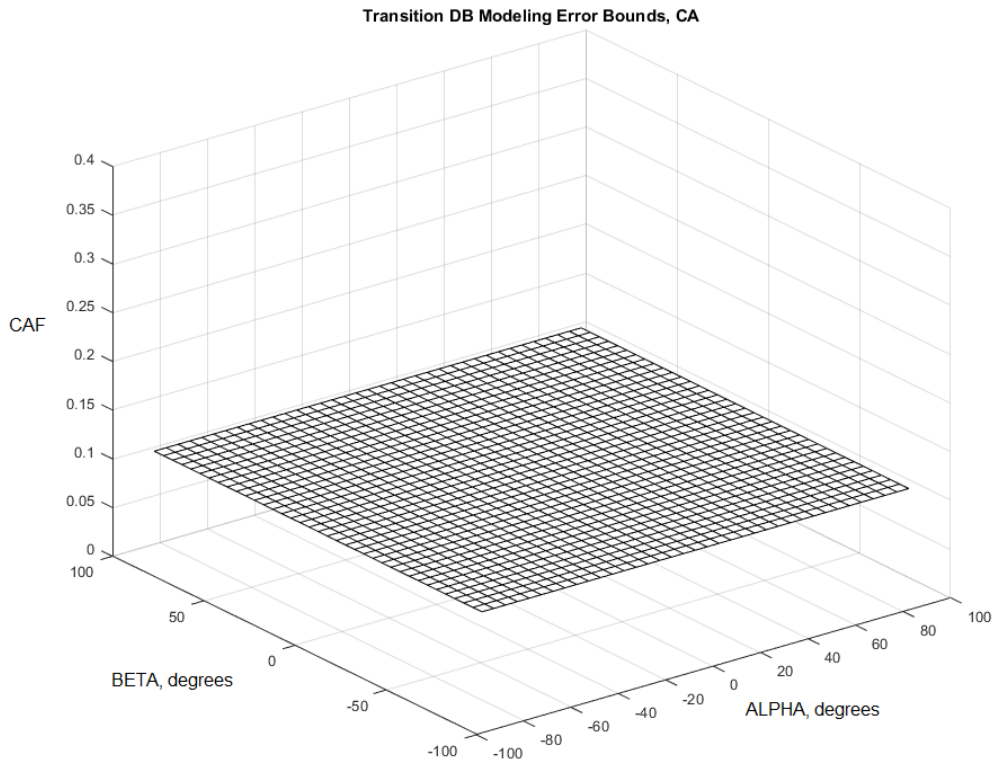

Figure 21. Transition database modeling error bounds for CAF in α-β space.

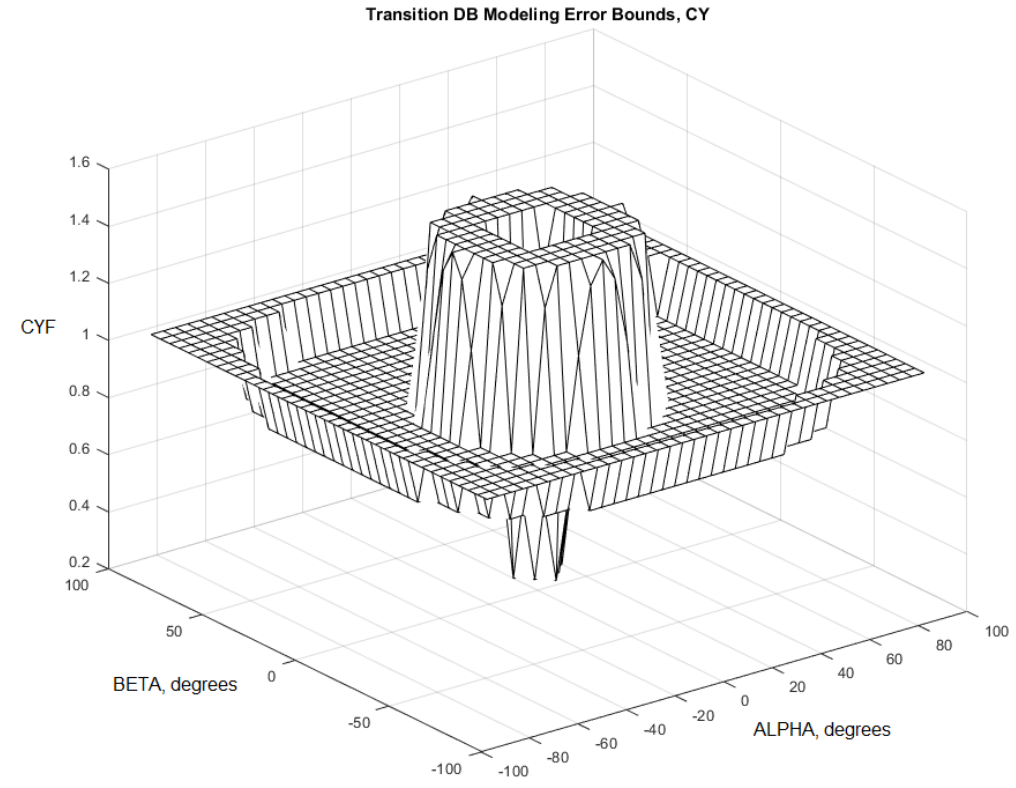

Figure 22. Transition database modeling error bounds for CYF in α-β space.

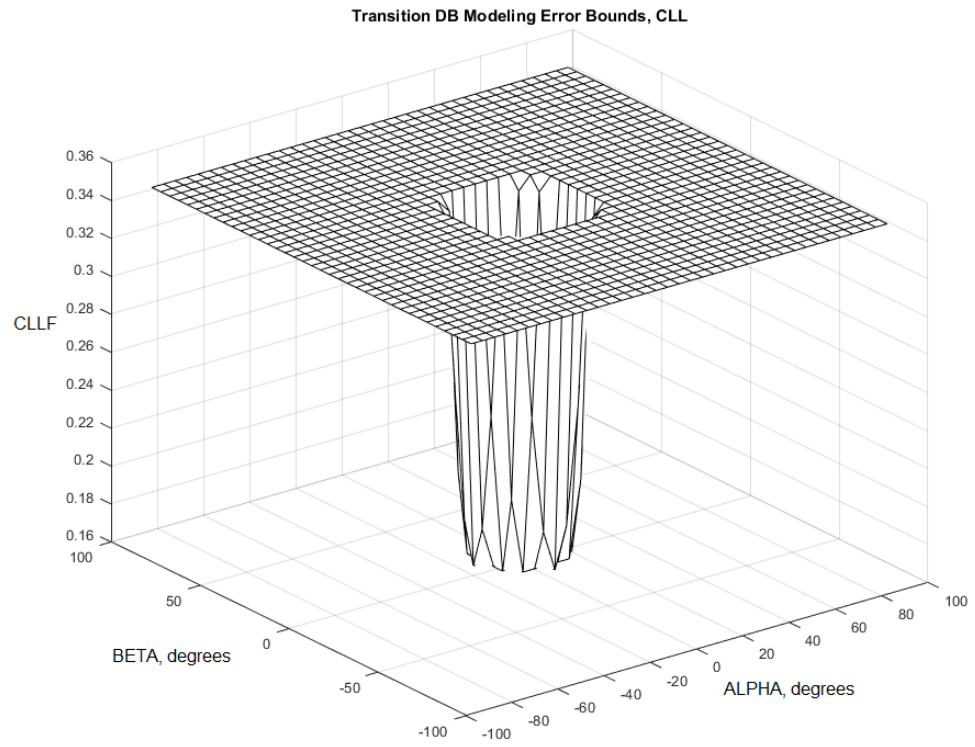

Figure 23. Transition database modeling error bounds for CLLF in α-β space.

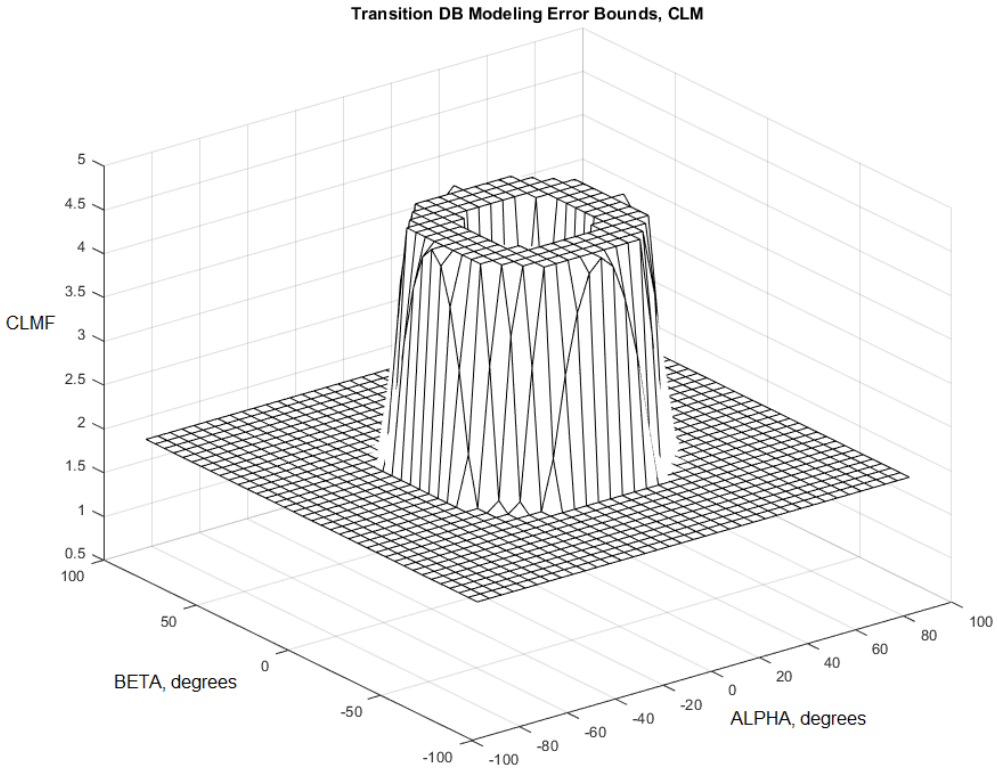

Figure 24. Transition database modeling error bounds for CLMF in α-β space.

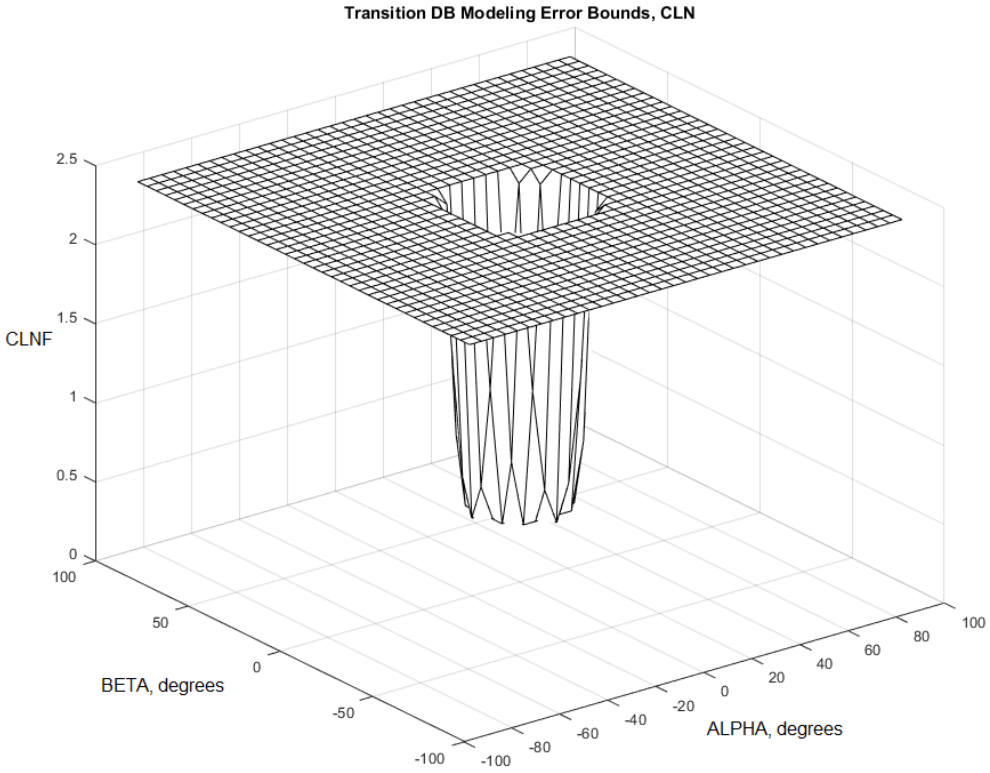

Figure 25. Transition database modeling error bounds for CLNF in α-β space.

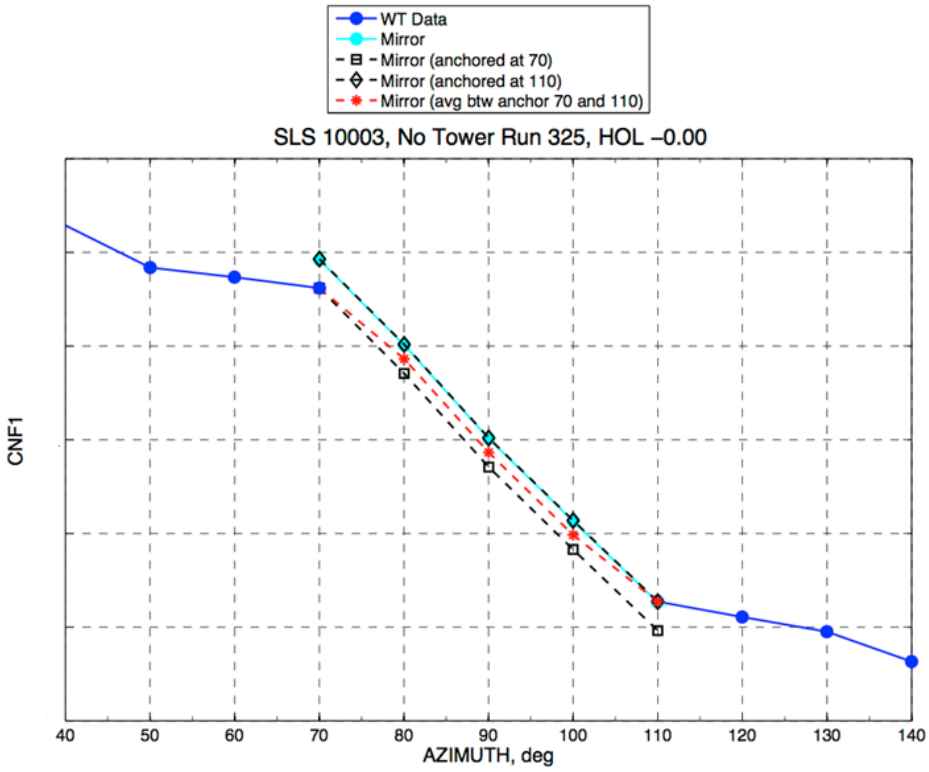

Figure 26. Illustration of process for computing tower effect increments at wind azimuth angles from 80° to 100°.

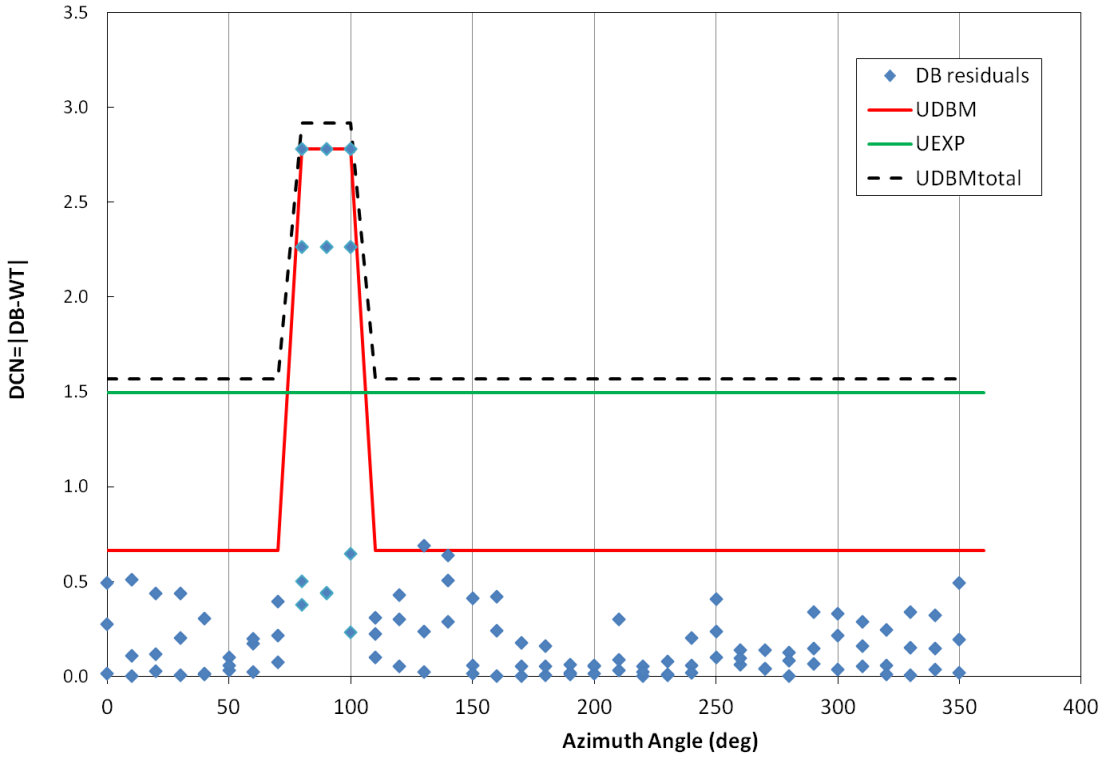

Figure 27. Database error buildup for tower increments of CNF.

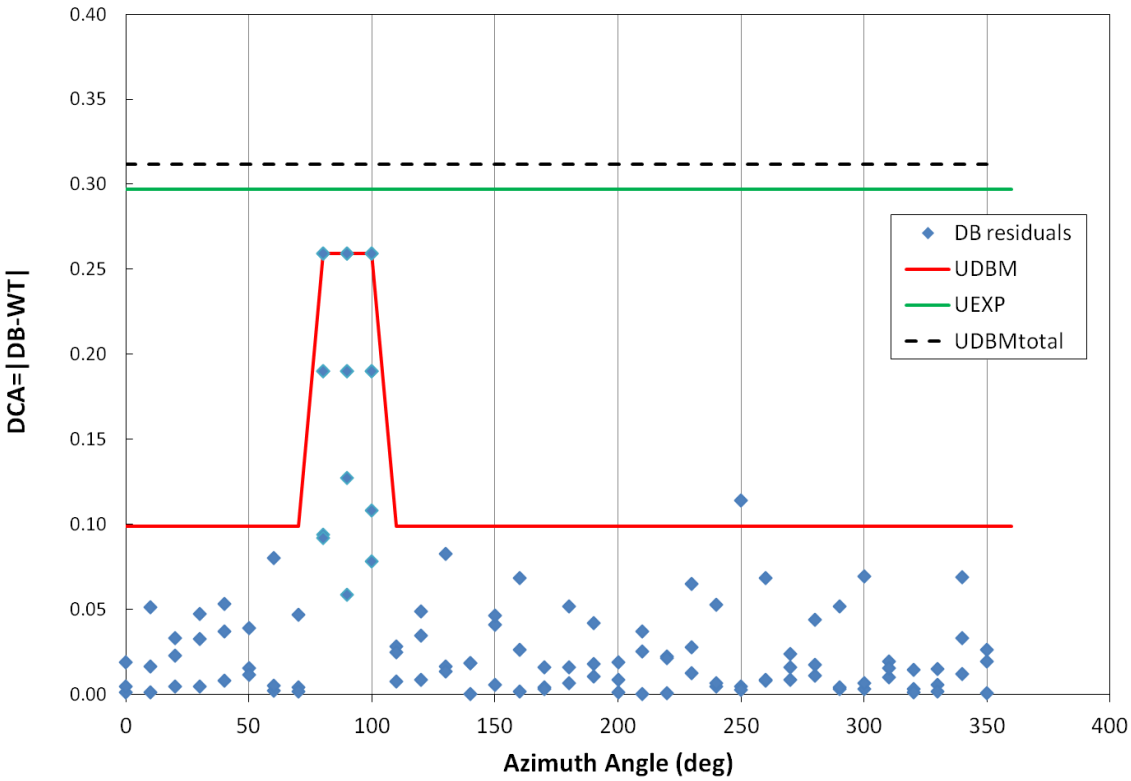

Figure 28. Database error buildup for tower increments of CAF.

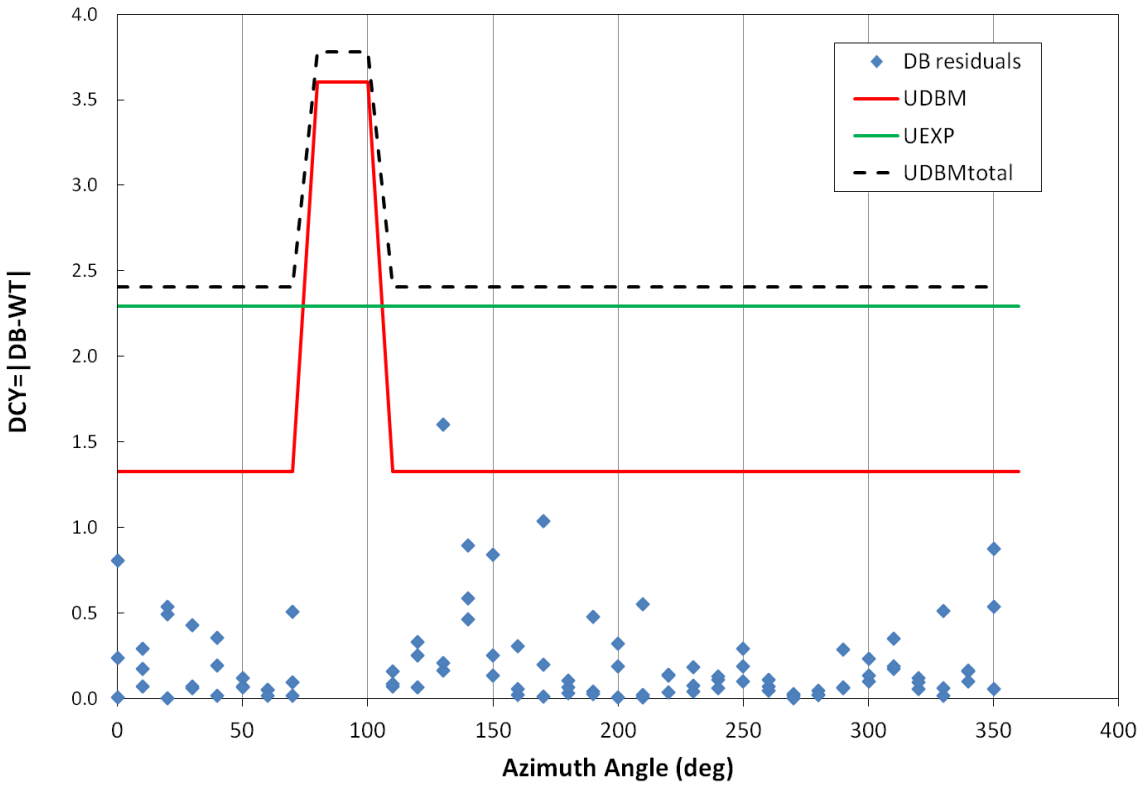

Figure 29. Database error buildup for tower increments of CYF.

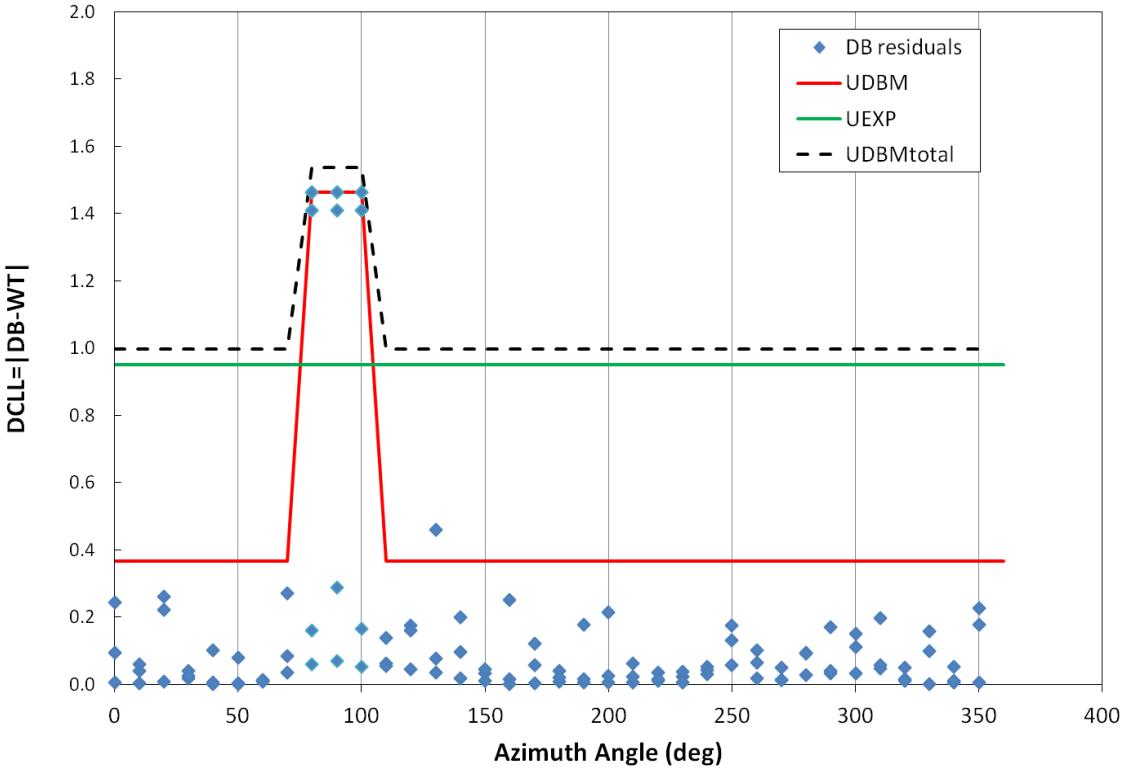

Figure 30. Database error buildup for tower increments of CLLF.

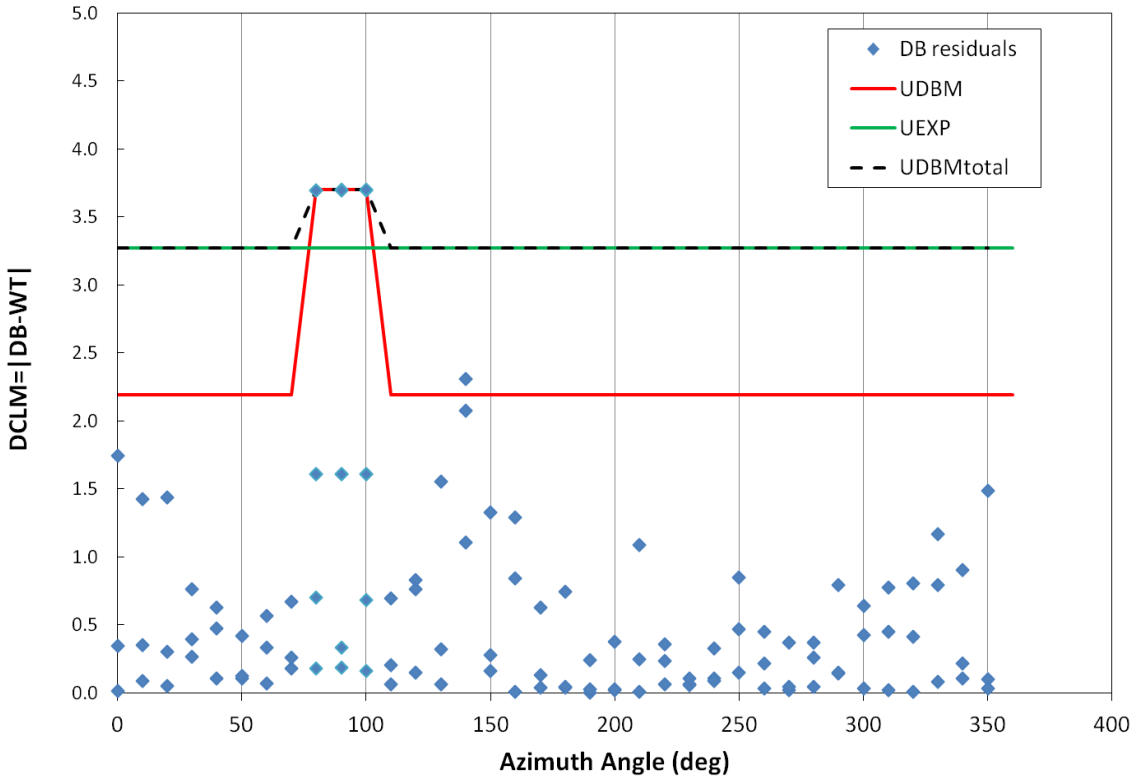

Figure 31. Database error buildup for tower increments of CLMF.

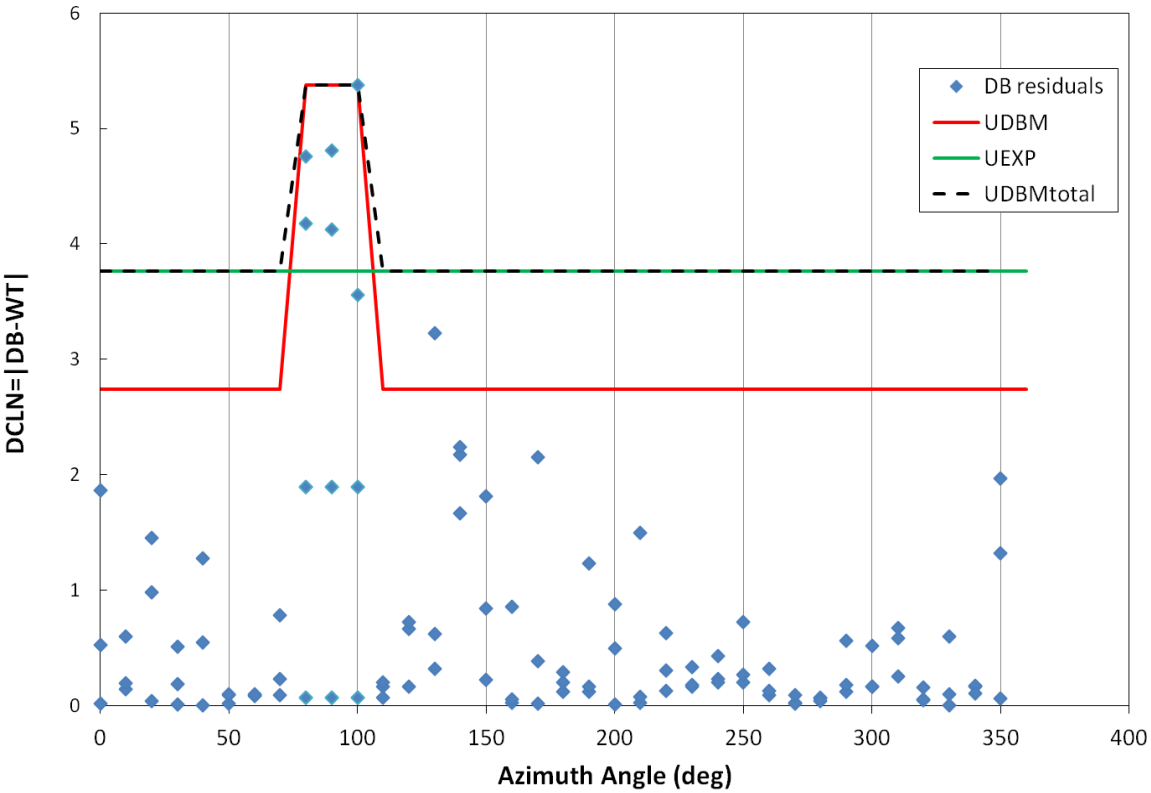

Figure 32. Database error buildup for tower increments of CLNF.

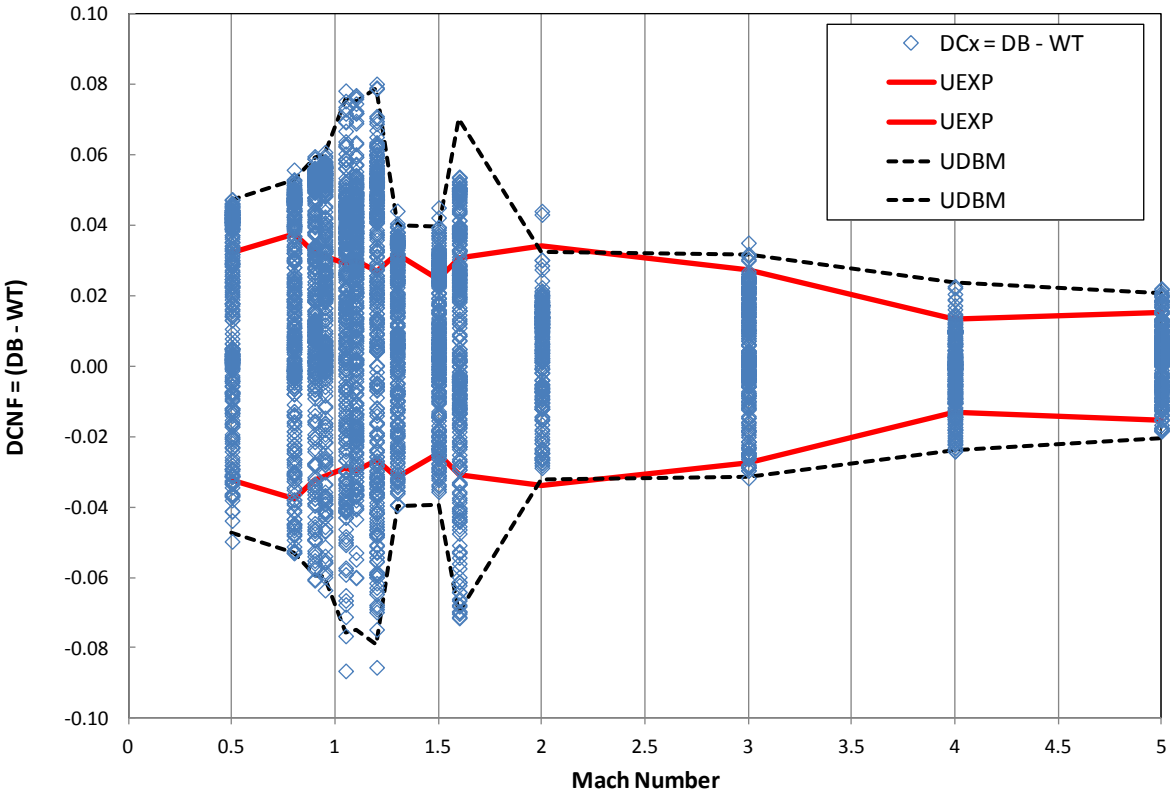

Figure 33. Ascent database modeling residuals and error bounds for CNF.

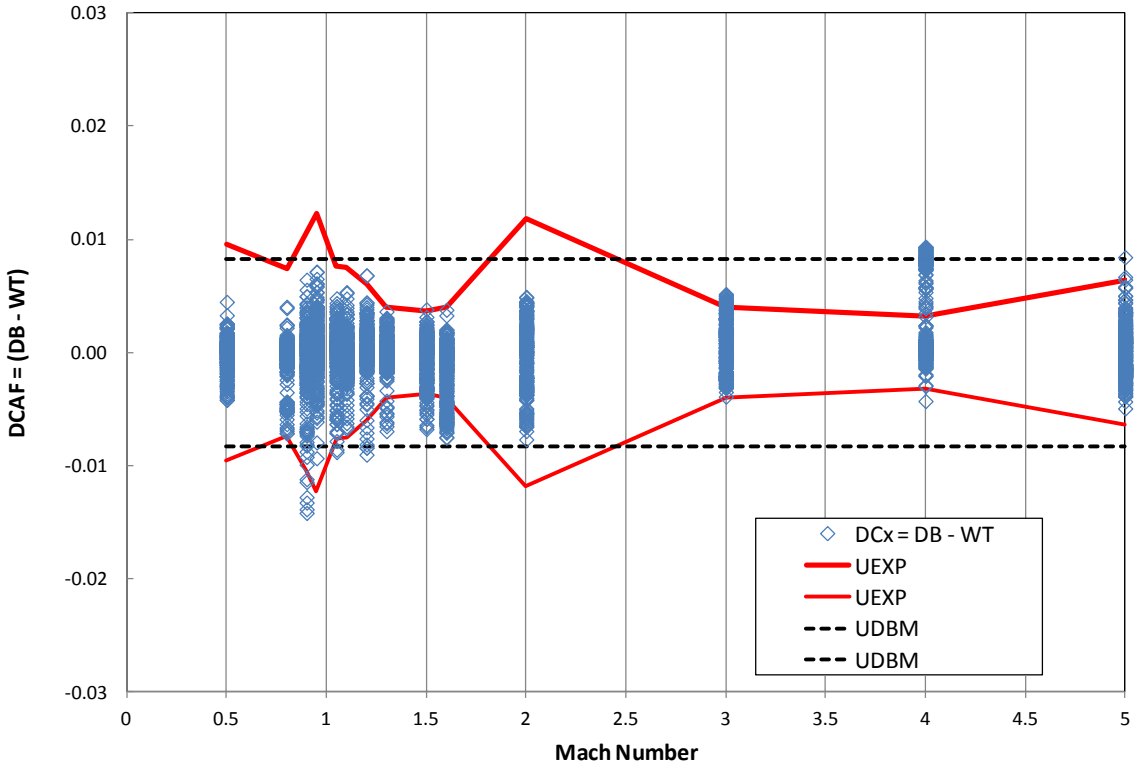

Figure 34. Ascent database modeling residuals and error bounds for CAF.

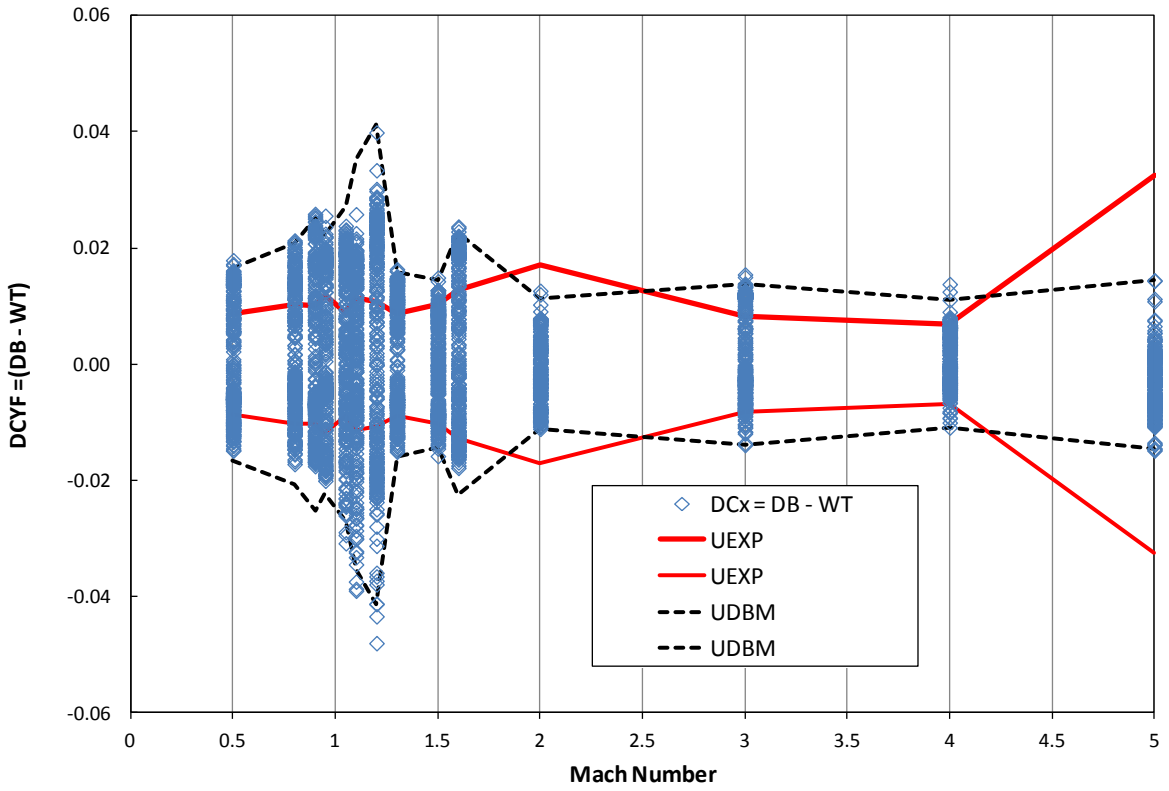

Figure 35. Ascent database modeling residuals and error bounds for CYF.

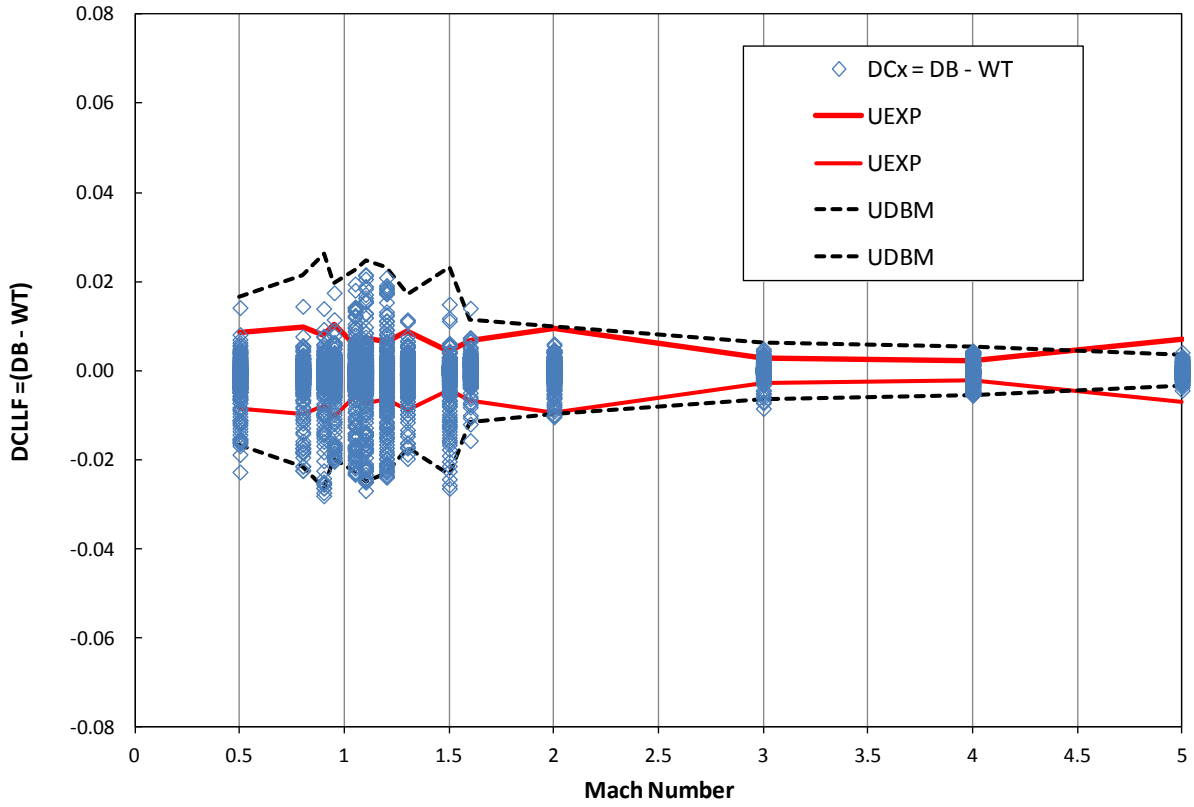

Figure 36. Ascent database modeling residuals and error bounds for CLLF.

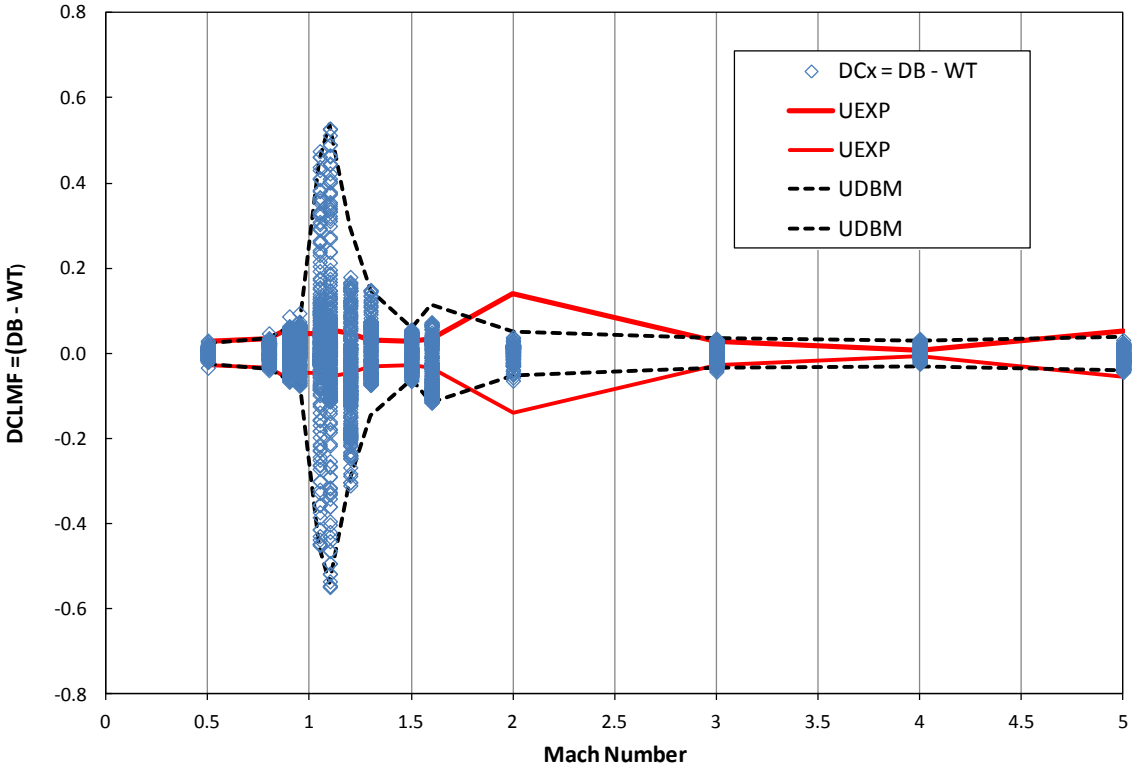

Figure 37. Ascent database modeling residuals and error bounds for CLMF.

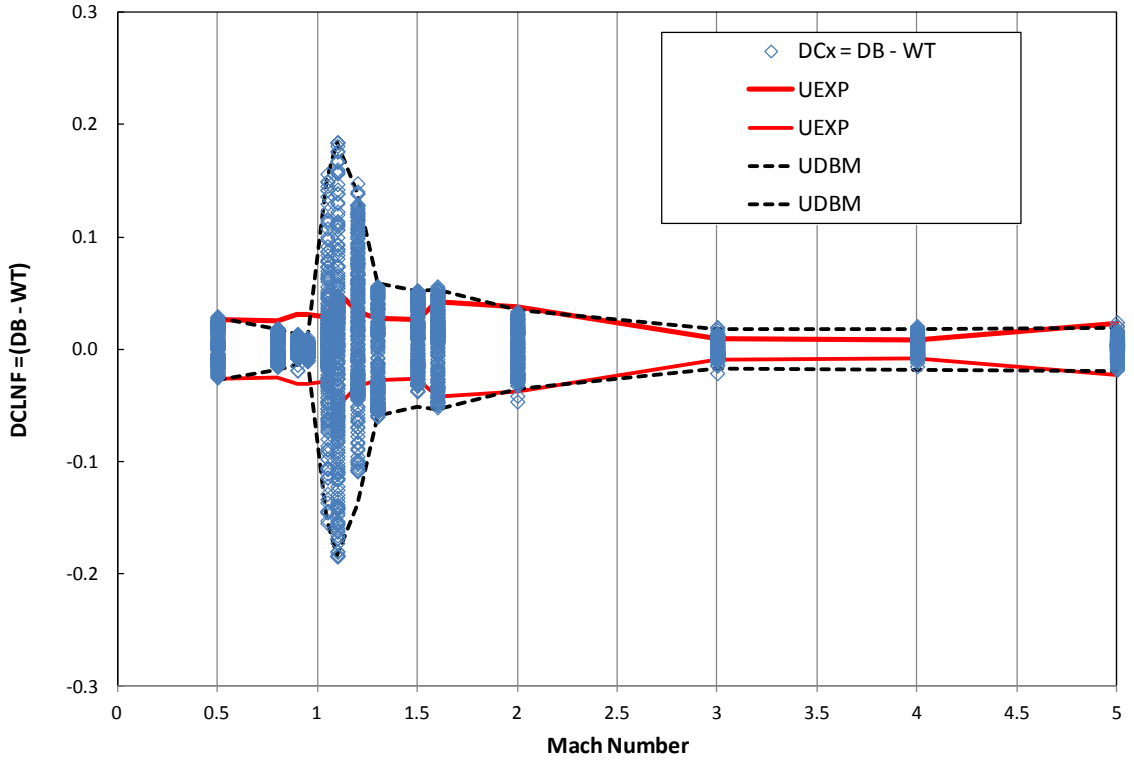

Figure 38. Ascent database modeling residuals and error bounds for CLMF.